The Origin of Hydrogen Bonding. An Energy Decomposition Study

Hideaki Umeyama and Keiji Morokuma*

Contribution from the Department of Chemistry, The University of Rochester, Rochester, New York 14627. *Received June 25, 1976*

Abstract: The energy decomposition analysis of Morokuma et al. within the ab initio SCF-MO theory has been applied to the study of the origin of hydrogen bonding. An examination of interaction energy components, electrostatic, polarization, exchange repulsion, charge transfer, and their coupling, for $(H_2O)_2$, $(HF)_2$, H_3N-HF, and other complexes in which the proton donor is HF, H_2O, NH_3, or CH_4 and the proton acceptor is HF, H_2O, and NH_3, as functions of geometric parameters, indicates these hydrogen-bonded complexes can be qualitatively called "electrostatic > charge transfer" or "electrostatic" complexes. The energy analysis of substituent effects in hydrogen bonding has been carried out for two examples, H_3N-HOZ where Z = H, CH_3, NH_2 and F, and RH_2N-HOH where R = H and CH_3, and is compared with those in electron donor-acceptor complexes and protonation complexes. A comparison of energy components with lithium complexes has been performed in two cases: $(LiF)_2$, $(LiH)_2$ with $(HF)_2$, and RH_2N-Li^+ with RH_2N-H^+. Based on these and our previous studies, the following questions concerning the origin of hydrogen bonding are discussed: (1) factors determining the geometrical parameters, in particular, the X-Y distance, the hydrogen bond directionality, and linearity, (2) energy components in hydrogen bond energy, (3) charge transfer and charge redistribution, (4) substituent effects, and (5) what makes hydrogen bonding unique?

I. Introduction

The results of many studies have been published on hydrogen bonding, concerning the structure of hydrogen bonded complexes, bonding characteristics, and spectroscopic properties.[1] Particularly important, but difficult, questions concern the origin of hydrogen bonding, i.e., the relative importance of electrostatic and charge transfer interactions in the stabilization, the reason why many hydrogen bonds are "linear" (meaning the X- - -H-Y segment is collinear), and factors which distinguish hydrogen bonding from other molecular interactions. In earlier days hydrogen bonding had been thought to be purely electrostatic in nature, a conjecture supported by the fact that electrostatic models often predict reasonable geometries for hydrogen bonded complexes. However, spectroscopic evidence has shown that the charge transfer interaction plays an important role as well. Similar questions have been asked concerning the origin of attraction in electron donor-acceptor (EDA) complexes[2] and molecular complexes which usually do not involve hydrogen bonding, and different viewpoints have been presented.[3]

Ab initio SCF molecular orbital (MO) theories have been extensively employed both for the prediction of the geometry and the stabilization energy of many hydrogen bonded complexes and for interpretation of the nature of the interaction. The systems studied include dimers and complexes of simple hydrides such as $(H_2O)_2$, $(HF)_2$, and H_3N-HF, polymers of hydrides, strongly hydrogen bonded complexes of cations and anions such as $H^+(H_2O)_n$ and $(FHF)^-$, hydrogen bonds in large organic compounds, and various excited states of hydrogen bonded complexes. Details of such theoretical studies have been reviewed recently[1b,4] and will not be reiterated here.

The energy and charge distribution decomposition (ECDD) analyses of Morokuma[5] and Kitaura-Morokuma[6] have proven to be a powerful method for direct analysis of the origin of molecular interactions.[7-15] Using model wave functions such as the partially antisymmetrized wave function or wave functions derived from a model Hartree-Fock matrix, which is obtained from the Hartree-Fock matrix by removal of specified matrix elements, individual components of the total interaction energy may be unambiguously defined within the Hartree-Fock method. The following separations of the energy stabilization ($\Delta E = E_{complex} - E_{monomers}$) and the charge distribution rearrangement ($\Delta\rho(r) = \rho(r)_{complex} - \rho(r)_{monomers}$) are possible.

$$\Delta E = ES + PL + EX + CT + MIX \quad (1)$$

$$\Delta\rho(r) = \rho_{PL}(r) + \rho_{EX}(r) + \rho_{CT}(r) + \rho_{MIX}(r) \quad (2)$$

The components are in accord with traditional viewpoints[16] and have the following physical meaning.

ES is the electrostatic interaction, i.e., the interaction between the undistorted electron distribution of a monomer A and that of a monomer B. This contribution includes the interactions of all permanent charges and multipoles, such as dipole-dipole, dipole-quadrupole, etc. This interaction may be either attractive or repulsive.

PL is the polarization interaction, i.e., the effect of the distortion (polarization) of the electron distribution of A by B, the distortion of B by A, and the higher order coupling resulting from such distortions. This component includes the interactions between all permanent charges or multipoles and induced multipoles, such as dipole-induced dipole, quadrupole-induced dipole, etc. This is always an attractive interaction.

EX is the exchange repulsion, i.e., the interaction caused by exchange of electrons between A and B. More physically, this is the short-range repulsion due to overlap of electron distribution of A with that of B.

CT is the charge transfer or electron delocalization interaction, i.e., the interaction caused by charge transfer from occupied MO's of A to vacant MO's of B, and from occupied MO's of B to vacant MO's of A, and the higher order coupled interactions.

MIX, the coupling term, is the difference between the total SCF interaction energy ΔE_{SCF} and the sum of the above four components and accounts for higher order interaction between various components.

In addition to the above components calculated within the Hartree-Fock scheme, there is a contribution of the correlation energy, which includes what is called the dispersion energy DISP. The contribution of the correlation energy to hydrogen bonding has not been widely studied.[4,17] However, apparent successes of the Hartree-Fock calculations and approximate calculations for simple systems suggest that it is relatively unimportant for interactions of small polar molecules as in hydrogen bonding. A second-order perturbation calculation using the 4-31G basis set by Lathan et al. gives an estimate of

the dispersion energy to be about 0.3–0.4 kcal/mol for $(H_2O)_2$ near the experimental and calculated equilibrium geometries and 0.9 kcal/mol for H_2CO–H_2O.[11] In the present paper, the effect of the correlation energy will not be considered.

The present ECDD analyses have been applied to many molecular interactions.[8] Morokuma[5] compared energy components for $(H_2O)_2$ and H_2CO–H_2O using an STO-3G basis set and concluded that ES, CT, and EX are all essential ingredients for hydrogen bonding, in accord with the classical empirical estimate of Coulson.[18] Iwata and Morokuma used ECDD analyses to analyze differences in hydrogen bonding energy between the ground and several low-lying excited states of H_2CO–H_2O,[7a] CH_2=$CHCHO$–H_2O,[7b] and $(HCOOH)_2$[15] and found that the major difference between states is often determined by ES, caused by the change in polarity of monomer molecules upon excitation. A comparison of ECDD analyses between different basis sets indicates that energy components are more sensitive to the basis set and that minimal basis set, such as STO-3G, will tend to overestimate the CT interaction, whereas double ζ-basis functions such as 4-31G are inclined to exaggerate the ES interaction. Qualitative conclusions obtained from ECDD analyses, however, have been found to be rather insensitive to the basis set.[8] Yamabe and Morokuma[9] defined the interaction electron density components (eq 2) and presented component density maps for the ground states of the hydrogen bonded complexes: $(H_2O)_2$, H_2CO–H_2O, and C_3H_2CO–H_2O. The maps, in conjunction with components of atomic electron population changes, give a visual appreciation of electron redistribution during the complex formation. They found that the largest redistribution of charge occurs via PL, which is the smallest energy component. (It should be noted that similar but less sophisticated energy and charge decomposition analyses have been carried out for a few limited systems independently by Kollman and Allen[19a] and by Dreyfus and Pullman[19b].)

The ECDD analyses have been applied also to many EDA complexes[8,10-13] and protonated bases.[14] The basis set dependence of the analyses has been examined, and a systematic study has been performed with one common basis set (i.e., 4-31G set) to facilitate a comparison between different complexes. Based on the attractive components making essential contributions to the stabilization of a complex at the equilibrium geometry, the EDA complexes studied have been very qualitatively categorized as follows:[13] H_3N–BF_3 and H_3N–BH_3, strong ES complexes; OC–BH_3, strong CT-PL-ES; H_3N–ClF and R_2O–$OC(CN)_2$, intermediate ES; HF–ClF, weak ES; H_3N–Cl_2 and H_3N–F_2, weak ES-CT; benzene–$OC(CN)_2$, weak ES-DISP; H_2CO–F_2 and H_2CO–C_2H_4, very weak CT-ES; and F_2–F_2, very weak DISP-CT. In addition the factors determining the equilibrium geometries of the various complexes have been identified. Though details depend on the complex and also on the deviation from the equilibrium, ES most often has been identified as the principal factor. The origin of alkyl substituent effects for several complexes also has been determined.[12-14] The substitution on an electron donor has increased the PL stabilization but at the same time increases the EX repulsion. The balance of the two determines the direction and the magnitude of the substituent effect; for instance, the *N*-alkyl substituent effect for H_3N–BH_3 is small because of the almost total cancellation of PL and EX, whereas for H_3N–H^+ the effect is large because EX does not exist (no electron on H^+) and PL is observed without cancellation. For a complex between ClF and HF, both the hydrogen bonded form ClF–HF and the non-hydrogen bonded form FCl–FH can exist and give an opportunity to compare the nature of hydrogen bonding and EDA interaction within a single complex. Both are found to be similar in energy, and the hydrogen bonded form is a weak ES-CT complex whereas the non-hydrogen bonded form is a weak ES or ES-CT complex.[13] The energy component which differs the most in the two forms is EX. The large EX in the hydrogen bonded complex may be attributed to the fact that the hydrogen atom of HF is more deeply buried in the electron cloud of the partner than any atom of the non-hydrogen bonded complex.

Since substantial progress has been made toward understanding the origin of EDA interaction, the time is ripe for similar systematic ECDD analyses of various hydrogen bonded complexes in order to elucidate the origin of hydrogen bonding. In the present paper we carry out ECDD analyses for hydrogen bonding between various combinations of HF, H_2O, NH_3, CH_4, and their derivatives. After a brief discussion on methods and geometries (section II), we examine in section III energy components of $(H_2O)_2$ as functions of various geometrical parameters to classify the complex based on the essential components and to identify the factors determining the geometry of the dimer. We also study the basis set dependence of the interaction energy and its components and analyze the components of orbital energy changes in the complex. Similar studies will be carried out for $(HF)_2$ in section IV and for H_3N–HF in section V. In section VI we compare the energy decomposition among eight hydrogen bonded dimeric complexes consisting of HF, H_2O, NH_3, and CH_4. Section VII will identify the origin of substituent effects in the hydrogen bonded complex H_3N–H_2O. Substituents on both the proton donor HOH and the proton acceptor H_3N will be examined. In section VIII we compare bonding in $(HF)_2$ with that in $(LiF)_2$ and $(LiH)_2$ in order to aid understanding of the unique nature of hydrogen bonding. In section IX summarizing the results of the preceding sections and previous papers we present the concluding discussions on the following questions[4b] concerning the origin of hydrogen bonding: (1) factors determining the geometry parameters of hydrogen bonded complex, in particular, the X–Y distance, the hydrogen bond directionality, and the linearity of the hydrogen bond; (2) energy components in hydrogen bond energy; (3) charge redistribution and charge transfer; (4) substituent effects in hydrogen bonding, proton affinity, and EDA interaction; (5) what makes the hydrogen bonding unique?

II. Methods and Geometries

All calculations of ΔE have been carried out within the closed shell LCAO-SCF-MO approximation. The GAUSSIAN 70 program[20] with our own ECDD analysis routines has been used. Unless otherwise noted, the 4-31G split-valence shell basis set with the recommended exponents, contraction coefficients, and scale factors,[21a] the same set used in our systematic studies of EDA complexes, has been used in all the calculations. In order to test the basis set dependence of ΔE and its components, we performed calculations for $(H_2O)_2$ and $(HF)_2$, using a less flexible, minimal basis set, STO-3G with standard parameters[21b] and a larger 6-31G** basis set which includes one set of polarization functions on each atom (a p function with the exponent $\alpha = 1.1$ for a hydrogen atom and a d function with $\alpha = 0.8$ for other atoms).[22] The IBMOLH program[23] has been used for the evaluation of the integrals for the 6-31G** set.

The ECDD analysis has been performed with the method of Kitaura and Morokuma.[6,24] The definitions of energy and charge distribution components and the mechanics of a calculation have been summarized in a recent publication[12] and will not be repeated here. In addition, we generalized the Kitaura–Morokuma method such that one can calculate more detailed components of CT. This extension of the method is such that interactions at the orbital level may be examined. This allows the following analyses to be performed: $CT_{A\rightarrow B}$ (charge transfer from A to B) and $CT_{B\rightarrow A}$, CT_σ (charge transfer through σ orbitals), and CT_π; $CT_{A\rightarrow B,\sigma}$ (charge transfer from A to B through σ orbitals) $CT_{A\rightarrow B,\pi}$, $CT_{B\rightarrow A,\sigma}$

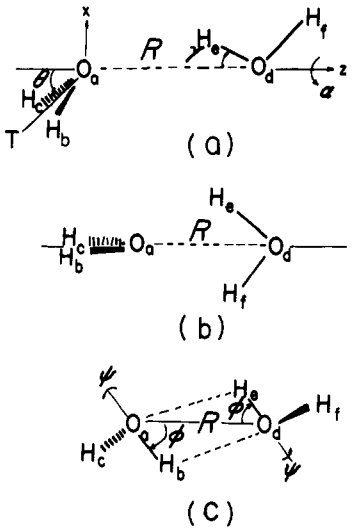

Figure 1. Geometry of three forms of $(H_2O)_2$: (a) linear form, (b) bifurcated form, and (c) cyclic form.

and $CT_{B\to A,\pi}$, $CT_{Ai\to B}$ (charge transfer from occupied MO_i of A to B). We have also established a method of calculating individual components of orbital energies:

$$E_i = E_i^0 + \Delta E_i = E_i^0 + E_{i'ES} + E_{i'PL} + E_{i'EX} + E_{i'CT} + E_{i'MIX} \quad (3)$$

where E_i^0 is the MO energy of isolated molecules and ΔE_i is the change induced by complexation. Details of the extension are given in the Appendix.

The geometries of the monomers were taken from experimental results, unless otherwise noted. HF, r(HF) = 0.9171 Å;[25] H_2O, C_{2v}. r(OH) = 0.956 Å, ∠HOH = 105.2°;[26] NH_3, C_{3v}, r(NH) = 1.0124 Å, ∠HNH = 106.67°;[26] CH_4, T_d, r(CH) = 1.094 Å;[26] CH_3OH; staggered, r(OH) = 0.967 Å, r(CO) = 1.428 Å, r(CH) = 1.098 Å, ∠HCH = 109.1°, ∠COH = 107.3°;[27] NH_2OH, staggered, r(NO) = 1.46 Å, r(OH) = 0.96 Å, r(NH) = 1.01 Å, ∠HON = 103°, ∠HNO = 105°, ∠HNH = 107°;[28] HOF, r(OH) = 0.964 Å, r(OF) = 1.442 Å, ∠HOF = 97.2°;[29] NH_2CH_3, C_s. staggered, r(CN) = 1.451 Å, $r(CH_2)$ = 1.109 Å, $r(CH_a)$ = 1.088 Å, ∠CNH = 110.9°, $\angle NCH_s$ = 111.7°, $\angle NCH_a$ = 110.1°, $\angle H_aCH_s$ = 108.1°, $\angle H_aCH_a$ = 108.6° (above from Me_3N),[30] and r(NH) = 1.0124 Å (from NH_3),[26] where H_s is on a symmetry plane and two H_a's are not. The geometry of the monomer is assumed to be retained in the complex, unless otherwise noted.

III. Water Dimer $(H_2O)_2$

The geometrical parameters for the "linear" hydrogen bonded $(H_2O)_2$ are defined in Figure 1a. The two oxygen atoms O_a and O_d are on the z axis and the bisector of $\angle H_bO_aH_c$, called T, is in the xz plane. The parameters are: $R = r(O_a\text{-}O_d)$, $\theta = \pi - \angle TO_aO_d$, α = the azimuthal angle of $H_eO_dH_f$ around the z axis with $\alpha = 0$ placing the molecule on the xz plane, and $\gamma = \angle H_eO_dO_a$ = rotation of $H_eO_dH_f$ around the y axis is a measure of the nonlinearity of $O_aH_eO_d$. Experimental values are R = 2.98 Å, θ = 60°, and $\alpha = \gamma = 0$.[31]

A. Basis Set Dependence. Since the interaction energy and its components depend on the basis set used, we at first compare the energy decomposition analysis for $(H_2O)_2$ at the experimental geometry mentioned above for the three basis sets, STO-3G, 4-31G, and 6-31G*. Table I shows these results, as well as calculated gross atomic populations and dipole moment of the monomer. The STO-3G basis gives a substantial overestimate of CT as compared with the other basis sets. This has been attributed to the lack of flexibility inherent in the minimum basis set; since the minimum set does not stabilize the individual molecules sufficiently, they utilize the vacant orbitals of the partner molecules to gain their stability, resulting in an unrealistically large CT stabilization.[7a,32] A comparison between 4-31G and 6-31G** results is interesting. The energy components EX and PL are almost indistinguishable between the two, whereas ES and CT stabilizations for the 4-31G set are larger than those for the 6-31G** set. The rationalization of this result centers on the fact that the ratios of the 4-31G ES and CT to those of the 6-31G** set are both found to be about 1.2, which is nearly equal to the ratio of the calculated dipole moment. Another point of view is that the difference in ES energy is large (~1.4 kcal/mol) whereas the difference in CT is insignificant (~0.3 kcal/mol). A similar comparison of basis sets for $(HF)_2$ to be presented in section IV suggests that the latter viewpoint is more generally applicable.

Table I. Basis Set Dependence of Energy Components in kcal/mol for Linear $(H_2O)_2$ at the Experimental Geometry[a] and Monomer Atomic Population N_H and N_O and Dipole Moment μ

	STO-3G	4-31G	6-31G**	Scaled[b]
ΔE	−5.1	−7.7	−5.6	−4.4
ES	−4.2	−8.9	−7.5	−6.3
EX	4.0	4.2	4.3	4.3
PL	−0.1	−0.5	−0.5	−0.5
CT	−4.8	−2.1	−1.8	−1.8
$CT_{PA\to PD}$	−4.8	−2.0	−1.7	
$CT_{PD\to PA}$	−0.01	−0.15	−0.15	
CT_σ		−2.1	−1.8	
CT_π		−0.03	−0.04	
MIX	0.1	−0.3	−0.1	−0.1
Monomer				
N_H	0.816	0.607	0.663	
N_O	8.369	8.787	8.675	
μ(D)[c]	1.72	2.60	2.2	

[a] R = 2.98 Å, θ = 60°, and $\alpha = \gamma = 0$. [b] ES is scaled down from 6-31G** results in proportion to the ratio of μ(exptl)/μ(6-31G**). [c] Experimental value 1.85 D.

Considering the fact that the 6-31G** set still overestimates the dipole moment (2.2 D calculated vs. 1.85 experimental), one can scale ES to a "correct" value of the dipole moment.[33] Such a scaled estimate of correct energy components is shown in the last column of Table I. The scaled ΔE = −4.4 kcal/mol agrees well with the most accurate SCF results (−3.9 ± 0.25 kcal/mol) of Popkie et al.[34] The scaled attractive energy is 72% ES, 21% CT, 6% PL, and 1% MIX, whereas the 4-31G attractive energy is 75% ES, 18% CT, 4% PL, and 3% MIX. Whether one uses 4-31G results, 6-31G** results, or scaled results, one concludes that the hydrogen bonded $(H_2O)_2$ may be qualitatively classified an "ES > CT complex" of an intermediate strength.

The relative importance of CT from the proton acceptor PA (electron donor) to the proton donor PD (electron acceptor) and that from PD to PA is an interesting question with regard to the nature and the origin of hydrogen bonding. As is discussed in the Appendix one can evaluate two terms separately by using an extension of the Kitaura-Morokuma decomposition method. The results of such a decomposition of CT contribution are shown in Table I. (The coupling CT term CT_{MIX} is so small that it is not listed.) Approximately 90% of the CT stabilization comes from the PA (electron donor) → PD (electron acceptor) charge transfer. It is also noted that the effect of a p orbital on hydrogen and a d orbital on oxygen atoms is very small.

Another method of further dividing the CT interaction is to consider CT through σ orbitals (PAσ → PDσ* and PDσ → PAσ*) and CT through π orbitals (PAπ → PDπ* and PDπ → PAπ*) separately. Here we refer to σ or π orbitals as being symmetric or antisymmetric with respect to the $TO_aO_dH_eH_f$

Table II. Energy Components in kcal/mol for Linear $(H_2O)_2$ as Functions of $R = r(O\text{-}O)$[a]

	R, Å						
	2.68	2.80	2.85	2.88[b]	2.90	2.98	3.28
ΔE	−6.9	−7.66	−7.78	−7.79	−7.78	−7.67	−6.5
Scaled[c]	*−2.3*	*−4.1*	*−4.5*	*-4.7_5*	*-4.8_2*	*−5.08*	*−4.8*
ES	−15.7	−12.3	−11.2	−10.5	−10.2	−8.9	−5.7
Scaled[c]	*−11.2*	*−8.7*	*−8.0*	*−7.5*	*−7.3*	*−6.3*	*−4.1*
EX	13.9	8.6	7.1	6.2	5.8	4.2	1.2
PL	−0.9	−0.7	−0.6	−0.6	−0.5	−0.5	−0.3
CL	−3.4	−2.7	−2.5	−2.4	−2.4	−2.1	−1.6
MIX	−0.7	−0.6	−0.5	−0.5	−0.4	−0.3	−0.1

[a] Other geometrical parameters from experiment: $\theta = 60°$ and $\alpha = \gamma = 0$ in Figure 1a. [b] Energy minimum from a rational fraction fit. [c] All italic entries are with a scaled ES which is 71% of ES calculated. See text.

Table III. Components in kcal/mol of MO Energy Changes upon Complex Formation for Linear $(H_2O)_2$ at the Experimental Geometry[a]

H_2O MO No. and symmetry[b]	1, a_1		2, a_1		3, b_2		4, a_1		5, b_1		6, a_1		7, b_2	
H_2O MO energy[c]	−20.5183		−1.3522		−0.7094		−0.5572		−0.4992		0.2090		0.3047	
Proton acceptor/donor[d]	PA	PD	PA	PD	PA	PD	PA	PD[e]	PA[e]	PD	PA	PD	PA	PD
ΔE[f]	−22	24	−21	22	−20	18	−23	27	−27	21	−16	34	−13	70
ES	−19	13	−17	15	−15	16	−20	13	−20	13	−10	15	−9	11
EX	2	3	0	1	0	−2	0	−3	9	2	9	−50	0	−25
PL	1	4	−0	2	−1	1	−0	2	1	3	−1	1	−1	1
CT	−15	3	−6	2	−6	2	−6	2	−6	2	−1	51	−3	70
MIX	9	0	2	0	1	−0	2	13	−11	1	−13	18	0	14

[a] $R = 2.98$ Å, $\theta = 60°$, and $\alpha = \gamma = 0$. [b] The first five monomer MO's are occupied. [c] Monomer MO energy in hartrees. [d] MO's assignable principally to the proton acceptor (PA) and donor (PD), respectively. [e] Mixing of these MO's is very extensive. [f] Every MO belonging to PA is shifted to a lower energy, whereas that of PD shifts to a higher energy.

plane of the molecule (the xz plane of Figure 1a with $\alpha = \gamma = 0$). The results of this analysis are also displayed in Table I. The principal result is that CT_π is negligibly small, and hence all of the CT that occurs is via the σ orbitals. Apparently the p_π orbital on the hydrogen atom is unable to play the role of a stepping stone between the two π electron systems. Since the exponent (1.1) is not fully optimized, the present results may be underestimating this role, but it is unlikely such an optimization will result in a severalfold increase in CT_π. Therefore, one must warn against a qualitative conclusion based on a semiempirical π electron MO theory or a qualitative argument based on the assumption that π electrons contribute to the CT stabilization of a hydrogen bond. A more detailed analysis of the CT component shows $CT_{\sigma,PA\rightarrow PD} = -2.00$ kcal/mol, $CT_{\sigma,PD\rightarrow PA} = -0.12$ kcal/mol. Furthermore, CT from an individual σ MO of PA to the vacant σ MO's of PD have been examined. The contributions are

PA, $\sigma MO1(1a_1,O_{1s}) \rightarrow$ PD: −0.03 kcal/mol
PA, $\sigma MO2(2a_1,OH_\sigma) \rightarrow$ PD: −0.06 kcal/mol
PA, $\sigma MO3(3a_1,O_n) \rightarrow$ PD: −1.42 kcal/mol
PA, $\sigma MO4(1b_1,O_\pi) \rightarrow$ PD: −1.16 kcal/mol

It is interesting to note that not the HOMO ($O\pi$ orbital of H_2O) but rather the second highest MO (O lone pair orbital of H_2O) is the largest contributor to the stabilization, that the lower orbitals do not contribute at all, and that the sum is larger than the $CT_{\sigma,PA\rightarrow PD}$ value of −2.00 kcal/mol, indicating that interactions of individual orbitals are not really separable but a strong coupling between them does take place.

As a compromise of flexibility and cost the 4-31G basis was exclusively used for the calculations of the following sections. We did, however, account for its consistent overestimate of the ES contribution.

B. Geometry Changes for Linear Hydrogen Bonding. We have examined, in some detail, the origin of the linear hydrogen bonding geometry, i.e., the reason the experimental geometry is as it is. We have carried out a series of calculations in which a single geometrical parameter at a time is varied from its experimental value, all other parameters remaining fixed at the experimental values.

The O-O distance R dependence of the energy components is shown in Table II. The flat curvature near the equilibrium R is principally due to cancellation of ES and EX. In order to correct for an exaggeration of ES in the 4-31G calculation, a scaling was carried out by multiplying ES by 0.71, the ratio of the H_2O dipole moment $\mu(exptl)/\mu(4\text{-}31G) = 1.85/2.60$. Scaled values of ES and ΔE obtained using ES_{scaled} with other unscaled components are shown in Table II in italics. The scaled ΔE has a minimum around 3.0-3.1 Å, in agreement with experiment (2.98 Å).

We have performed the decomposition analysis of MO energies, as described in the Appendix, at the experimental geometry. The results are shown in Table III and Figure 2. All the MO energies of the proton donor (PD) increase, whereas those of the acceptor (PA) decrease by about 20-30 kcal/mol for occupied orbitals and more for vacant orbitals. These changes are essentially determined by ES for most orbitals. That is to say, the lowering of the PA's MO energies occurs just because its electrons feel the attractive electrostatic potential of PD, and the increase of the PD's MO energies takes place simply by the repulsive electrostatic potential due to PA. For occupied MO's, CT makes a secondary contribution reenforcing the ES contribution. The strong PA → PD,CT interaction causes a mixing of PA's occupied MO's with the PD's vacant MO's, resulting in the stabilization of the former and a large destabilization of the latter. As was outlined in an earlier paper,[12] the EX interaction consists of two parts. First there is the contribution of exchange integrals ($-\Sigma K_{ij}$) between the MO's of the PA and the PD. Usually $K_{ij} > 0$, and hence this contribution is generally attractive. In addition there is a contribution of the overlap between occupied MO's of PA and PD. The deformation of occupied MO's to satisfy the Pauli principle destabilizes the electrons, giving a repulsive energy contribution. Usually the second term is larger than the first, resulting in a net exchange repulsion in the total energy. For

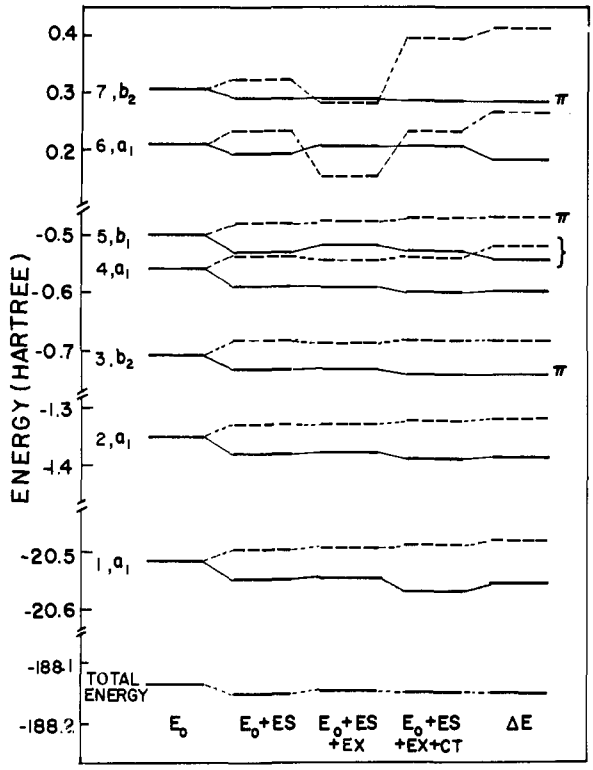

Figure 2. MO energy and total energy components in linear $(H_2O)_2$ at the experimental geometry. The MO number and symmetry are for monomer. The MO's belonging principally to the proton acceptor are given by solid lines and those of the proton donor by broken lines. The two MO's between −0.5 and −0.55 hartree mix so strongly that assignments are rather qualitative. The π(a″) MO's of the dimer are marked as such on the right edge; all other MO's are σ(a′) MO's.

orbital energies, such a simplified generalization is not necessarily applicable. Both positive and negative EX are found in Table III. For vacant orbitals, the overlap term becomes attractive as well as the exchange integral term, making EX a large attractive interaction.

Next, we examined the energy components as functions of θ as defined in Figure 1a, the results being given in Table IV. ΔE has a minimum around 35° (quadratic fit of values at 15, 45, and 60°).[35] The ES, by itself, also has a maximum stabilization around 35°. The CT stabilization and the EX repulsion both increase monotonically with θ, while the largest PL contribution for $\theta = 0$ occurs. the magnitude of change between $\theta = 0$ and 75° is rather comparable among the various components: 0.9 for ES, 0.6 for EX, 0.3 for PL, and 0.9 kcal/mol for CT. As is seen in Figure 2, the highest occupied MO of H_2O is a $\pi(b_1)$ orbital, which is perpendicular to the molecular plane $H_bO_aH_b$ (Figure 1a). The overlap between this orbital and the σ and σ^* orbitals of the proton donor H_2O is largest when $\theta = 90°$. Apparently, in determining the preferred angle θ for CT and EX this π orbital plays a more important role than the second highest occupied, n-type (a_1) orbital, which is in the plane of $H_bO_aH_c$ and hence would prefer that $\theta = 0°$. Since the angular dependence of the attractions CT + PL is almost completely cancelled by that of the repulsion, EX, the behavior of ΔE appears to be controlled solely by ES. The angular dependence of ES cannot be explained if each H_2O is considered to be a point dipole.

A fractional charge model has recently been proposed by Noell and Morokuma for ab initio calculations of the electronic structure of a molecule in solutions and crystals.[36] This is similar to the model used by Stillinger and Rahman for their statistical studies of the structure of liquid water.[37] In this model a solvent H_2O molecule is represented by three fractional point charges, $+\delta$ on each hydrogen atom and -2δ on the oxygen atom. The fractional charge model takes into account the quadrupole as well as the dipole moment of the H_2O molecule. In order to examine whether the angular dependence of the interaction energy between two water molecules can be reproduced by the purely classical electrostatical interaction between these fractional charges, we have carried out a complete geometry optimization for relative orientation of the H_2O molecules with a fixed monomer geometry and O–O distance. Regardless of whether we use $\delta = 0.332$ or 0.466 which reproduce the experimental and 4-31G calculated dipole moments, 1.85 and 2.60 D, respectively, the optimized geometry is a "linear hydrogen bond" complex of Figure 1a with $\theta \sim 20°$, $\gamma \sim -5°$, and $\alpha \sim 0°$. This is the only minimum obtained in this model; an optimization starting from bifurcated and cyclic structures also converged to the above linear structure. Though the optimized value of $\theta \sim 20°$ is smaller than the value $\theta \sim 35°$ from the ES component of the 4-31G ab initio energy (Table IV), otherwise the geometry predicted by the simple fractional charge interaction is in good agreement with that predicted by ab initio calculations and with experimental results.

The dependence of energy components on the azimuthal angle α as defined in Figure 1a was examined and the results are shown in Table V. $\alpha = 0$ and 180° correspond to the trans and cis configuration, respectively, for $TO_aO_dH_f$: ES is the component keeping the atoms $O_aH_eO_dH_f$ from going out of plane.

In order to examine the origin of linearity of the $O_aH_eO_d$ hydrogen bond axis, the proton donor $H_eO_dH_f$ is rotated around the y axis with O_d at the center by γ (Figure 1a). Results in Table VI indicate that $\gamma = +10°$ can be accomplished without much loss of energy, because a reduction in ES and CT stabilization is compensated by a decrease in EX repulsion. For $\alpha = -10°$, a reduction in EX is not sufficient to balance a loss in ES. The loss in ES for both cases is consistent with the fractional change model discussed in a preceding paragraph. The linear structure is most preferred due to a short distance O_a–H_e attraction and the deviation $\gamma > O$ is favored over $\gamma < 0$ because $\gamma > 0$ reduces the $H_b^{+\delta}$– and $H_c^{+\delta}$–$H_e^{+\delta}$ repulsion.

Table IV. Energy Components in kcal/mol for Linear $(H_2O)_2$ as Functions of θ[a]

	θ				
	0°	15°	45°	60°	75°
ΔE	−7.4	−7.7	−7.9	−7.7	−7.1
ES	−8.7	−9.0	−9.2	−8.9	−8.3
EX	3.7	3.7	4.0	4.2	4.3
PL	−0.6	−0.6	−0.5	−0.5	−0.4
CT	−1.5	−1.6	−1.9	−2.1	−2.4
MIX	−0.2	−0.2	−0.3	−0.3	−0.4

[a] Other parameters from experiment: R = 2.98 Å and $\alpha = \gamma = 0$ in Figure 1a.

Table V. The Azimuthal Angle α Dependence of Energy Components in kcal/mol for Linear $(H_2O)_2$[a]

	α		
	30°	90°	180°
$\Delta\Delta E$	0.2	1.4	2.3
ΔES	0.2	1.3	2.4
ΔEX	0.0	0.0	−0.0
ΔPL	−0.0	0.0	0.0
ΔCT	0.0	0.0	−0.0
ΔMIX	−0.0	−0.0	−0.0

[a] Other parameters from experiment: R = 2.98 Å, θ = 60°, and γ = 0 in Figure 1a. The energy is the difference from α = 0.

Table VI. The Effect of Nonlinearity of the Hydrogen Bond Axis O- - -H-O on Energy Components in kcal/mol for Linear $(H_2O)_2$[a]

	γ	
	−10°	10°
ΔΔE	0.5	0.1
ΔES	0.5	0.2
ΔEX	−0.1	−0.4
ΔPL	0.1	−0.0
ΔCT	0.0	0.1
ΔMIX	0.0	0.1

[a] γ is the angle of deviation from the linearity of O- - -H-O as defined in Figure 1a. Other parameters from experiment: R = 2.98 Å, θ = 60°, and α = 0. The energy is the difference from γ = 0.

Table VII. Energy Components in kcal/mol for Bifurcated $(H_2O)_2$ as Functions of $R = r(O\text{-}O)$[a]

	R, Å[b]					
	2.68	2.80	2.85	2.90	2.98	3.28
ΔE	−5.7	−6.33	−6.41	−6.44	−6.37	−5.5
Scaled[c]	*−2.9*	*−3.9*	*−4.1*	*−4.30*	*−4.43*	*−4.1*
ES	−9.8	−8.3	−7.8	−7.4	−6.7	−5.0
Scaled[c]	*−7.0*	*−5.9*	*−5.6*	*−5.2*	*−4.8*	*−3.6*
EX	5.9	3.6	2.9	2.3	1.7	0.4
PL	−0.4	−0.3	−0.3	−0.3	−0.3	−0.2
CT	−1.2	−1.1	−1.0	−1.0	−1.0	−0.8
MIX	−0.2	−0.1	−0.1	−0.1	−0.1	−0.0

[a] Geometry specified in Figure 1b. [b] A rational fraction fit gives the energy minimum at R = 2.90 Å. [c] All italic entries are with a scaled ES which is 71% of ES calculated.

Table VIII. Energy Components in kcal/mol for Cyclic $(H_2O)_2$ as Functions of $R = r(O\text{-}O)$[a]

	R, Å[b]					
	2.68	2.80	2.85	2.90	2.98	3.28
ΔE	−5.6	−6.1	−6.12	−6.10	−5.9	−4.8
Scaled[c]	*−2.6*	*−3.7*	*−4.0*	*−4.13*	*−4.22*	*−3.7*
ES	−10.3	−8.1	−7.4	−6.8	−5.9	−3.8
Scaled[c]	*−7.3*	*−5.8*	*−5.2*	*−4.08*	*−4.2*	*−2.7*
EX	9.3	5.7	4.7	3.8	2.8	0.8
PL	−0.5	−0.4	−0.3	−0.3	−0.2	−0.1
CT	−3.5	−3.0	−2.8	−2.6	−2.3	−1.6
MIX	−0.5	−0.4	−0.3	−0.3	−0.2	−0.1

[a] Geometry specified in Figure 1c with ϕ = 40° and ψ = 50°. [b] A rational fraction fit gives the energy minimum at R = 2.85 Å. [c] All italic entries are with a scaled ES which is 71% of ES calculated.

The loss in CT for $\gamma > 0$ is due to a loss in the overlap between the π orbital and the proton acceptor and the O_d-$H_e\sigma^*$ orbital. A decrease in EX is caused by a loss of contact between the electron cloud of O_a and the hydrogen bonding proton H_e. $\gamma > 0$ is better than $\gamma < 0$ for EX, because the former puts the proton further away from the electron cloud of the proton acceptor molecule.

If one rotates the proton donor molecule $H_eO_dH_f$ around the y axis with H_e at the center, instead of O_d, a large destabilization will result due mainly to a loss of ES and an increase in EX repulsion caused by a decrease in the O_aO_d distance.

C. Bifurcated and Cyclic Structures. Three plausible structures of the water dimer (linear (Figure 1a), bifurcated (Figure 1b), and cyclic (Figure 1c)) have been compared by Morokuma and Pedersen[38] and by Kollman and Allen.[39] The linear structure has been found to be the most stable and is also the only structure to be experimentally observed.[31] In order to shed light on the reason why this is the case, the energy decomposition analysis has been carried out for bifurcated and cyclic dimers. In the bifurcated structure (Figure 1b) the proton donor H_2O is assumed to be perpendicular to the acceptor H_2O, maintaining the overall C_{2v} symmetry. Energy components, as well as the scaled ES (×0.71) and ΔE, as functions of the O_a-O_d distance R, are shown in Table VII. The cyclic structure (Figure 1c) is assumed to have a center of inversion and is specified by $\phi = \angle O_dO_aH_b = \angle O_aO_dH_e$, ψ = the rotation angle of H_c around the O_aH_b axis = the rotation axis of H_f around the O_dH_e axis, and R = the O_a-O_d distance. Kollman and Allen's optimized values ϕ = 40° and ψ = 50° are assumed. Energy components and the scaled ES and ΔE as functions of R are shown in Table VIII. Potential curves for both bifurcated and cyclic structures are flatter near the equilibrium R_e than is the surface for the linear structure (Table V). This plateau in the surface is obviously due to the almost complete cancellation in the R dependence of ES and EX, whereas in the linear structure EX repulsion increases more rapidly than ES as R decreases. In both bifurcated and cyclic structures the major source of the EX repulsion should be the contact of electron clouds between O_a and O_d, while in the linear structure it is between O_a and H_e. An oxygen atom has an electron cloud more widely spread out and therefore less dense in the contact region, therefore giving rise to a "softer" less steep repulsive wall than a hydrogen atom would.

Table IX compares the energy components at the calculated R_e as well as at R_e obtained from the scaled ΔE between three structures. The scaled R_e values for various structures are less accurately determined than the unscaled ones since fewer points are available but appear to be almost identical within ±0.02 Å. Regardless of whether one uses the 4-31G results or the scaled results, one concludes that the principal reason why the linear geometry is preferred is the ES contribution. Between the linear and bifurcated structure, CT as well as ES favors the linear while EX prefers the bifurcated. As was discussed in section IIIB, a simple fractional charge model of ES

Table IX. Comparison of Energy Components in kcal/mol at the Calculated R_e for Three Structures of $(H_2O)_2$

	4-31G			4-31G scaled[a]		
	Linear	Bifurcated	Cyclic	Linear	Bifurcated	Cyclic
R_e, Å	2.88	2.90	2.85	~2.98	~2.98	~2.98
ΔE	−7.8	−6.4	−6.1	−5.1	−4.4	−4.2
ES	−10.5	−7.4	−7.4	−6.3	−4.8	−4.2
EX	6.2	2.3	4.7	4.2	1.7	2.8
PL	−0.6	−0.3	−0.3	−0.5	−0.3	−0.2
CT	−2.4	−1.0	−2.8	−2.1	−1.0	−2.3
MIX	−0.5	−0.1	−0.3	−0.3	−0.1	−0.2

[a] Used ΔE_{scaled} which employs ES_{scaled} = 71% of calculated ES.

Table X. Energy Components in kcal/mol for Linear $(HF)_2$ of $R = r(F\text{-}F)$ and Its Basis Set Dependence

	Linear,[a] R, Å						Cyclic,[b] R, Å
	2.49	2.69	2.71[c]	2.79	3.09	2.79[d] (4-31G**)	2.88
ΔE	−6.4	−7.59	−7.60	−7.48	−6.1	−6.4	−5.6
Scaled[e]	*−3.9*	*−5.88*	*−5.94*	*−6.04*	*−5.1*		*−4.8*
ES	−12.6	−8.5	−8.2	−7.2	−4.7	−6.0	−3.9
Scaled[e]	*−10.1*	*−6.8*	*−6.6*	*−5.7*	*−3.7*		*−3.1*
EX	11.9	4.9	4.5	3.1	0.8	3.2	0.7
PL	−0.8	−0.4	−0.4	−0.3	−0.2	−0.5	−0.1
CT	−4.3	−3.3	−3.2	−2.9	−2.0	−3.0	−2.2
MIX	−0.5	−0.3	−0.3	−0.2	−0.0	−0.1	−0.1

[a] Other geometrical parameters from experiment: $\theta = 60°$ and $\gamma = 0$ in Figure 3a. [b] $\phi = 54.5°$ after Kollman and Allen (Figure 3b). [c] Energy minimum obtained from a rational fraction fit. [d] This column only with the 4-31G** basis set. All others with the 4-31G set. [e] All italic entries are with a scaled ES which is 80% of ES calculated. See text.

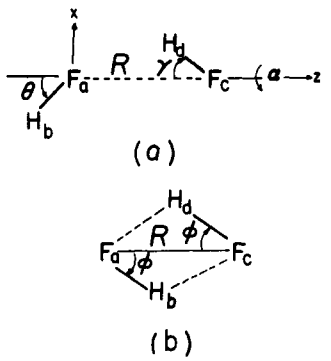

Figure 3. Geometry of two forms of $(HF)_2$: (a) linear form, and (b) cyclic form.

interaction yields a preference for a linear structure. The loss of CT in the bifurcated structure is probably due to the loss of overlap between the π and n orbitals of the proton acceptor and the σ^* orbitals of the donor. The reason why EX prefers the bifurcated has been given in the preceding paragraph. Comparing between the linear and cyclic structure, one finds that ES favors the linear and EX favors the cyclic, while CT is very similar for the two structures. The following argument can be made. The overlap between the π and n orbitals of the proton acceptor oxygen O_a with the σ^* orbitals of the proton donor for the cyclic structure is obviously less favored than for the linear structure but is not as bad as the bifurcated structure. One also must recognize that while the linear structure has one hydrogen bond, the cyclic structure has two, in which each molecule acts as a proton donor for one bond and as a proton acceptor for the other. This head-tail-head-tail type cyclic interaction should be a favorable situation for charge delocalization between molecules. Apparently a complicated balance of these factors keeps CT unchanged between the linear and cyclic structure. Summarizing the comparison of structures in this section and a study of nonlinear deviation of a linear structure in section IIIB, one may conclude that a hydrogen bonded complex tends to maintain a linear X- - -H-Y hydrogen bond principally to achieve the maximum ES stabilization which is the most important component of the hydrogen bond energy.

IV. Hydrogen Fluoride Dimer $(HF)_2$

The geometrical parameters for the "linear" hydrogen bonded $(HF)_2$ are defined in Figure 3a. The two fluorine atoms F_a and F_c are on the z axis and the hydrogen atom H_b is on the xz plane. The parameters are: $R = r(F_a\text{-}F_c)$, $\theta = \pi - \angle H_bF_aF_c$, $\gamma = \angle H_dF_cF_a$, and α = the azimuthal angle of H_dF_c around the z axis with $\alpha = 0$ placing the molecule H_dF_c on the xz plane. Experimental values are $R = 2.79$ Å, $\theta = 60°$, and $\gamma \simeq 0$.[40]

A. Basis Set Dependence. Columns 5 and 7 of Table X show the energy components of the hydrogen bond energy of $(HF)_2$ at the experimental geometry using the 4-31G and the 4-31G** basis set. The difference between the two columns is small except for ES, indicating that ES is overestimated by the 4-31G set, but other components are not sensitive to an improvement of the basis set. Since the experimental dipole moment (1.83 D) of the HF monomer is 80% of the 4-31G calculated dipole 2.28 D, a scale factor of 0.80 can be used, as in $(H_2O)_2$ (section IIIA), to calculate a "corrected" or scaled ES from the 4-31G value. In the following discussions we consider only the 4-31G and the scaled 4-31G values.

B. Geometry Changes for Linear Hydrogen Bonding. We have performed a series of calculations in which geometrical parameters for the linear structure are varied one by one from the experimental values. The F-F distance R dependence of energy components is also given in Table X. The 4-31G minimum is $R = 2.71$ Å, whereas the scaled ΔE gives $R \sim 2.79$ Å which is equal to the experimental value. When compared at the experimental R, both the 6-31G** and 4-31G** calculations and the scaled 4-31G ΔE suggest that $(HF)_2$ is probably a slightly stronger complex than $(H_2O)_2$. $(HF)_2$ has a smaller ES stabilization but a substantially smaller EX repulsion and a larger CT stabilization. The smaller ES for $(HF)_2$ than for $(H_2O)_2$ may be understood by considering a local electron distribution on the proton and the proton acceptor. For HF, if the formal charge on H is $+\delta$, F has the charge $-\delta$. The ES interaction between the proton and the proton acceptor at a distance R will very approximately be $-\delta^2/R$. For H_2O, if the formal charge on H is $+\delta$, O has the charge -2δ. The approximate ES interaction between H and O will be $-2\delta^2/R$. Though the proton charge δ for HF is presumably larger than that for H_2O, the factor of 2 in the formal charge of the oxygen will result in a larger ES contribution for the H_2O dimer than for the HF dimer. For instance, if one uses the 4-31G gross populations $\delta(HF) = +0.48$, $\delta(H_2O) = +0.39$, and $R(H\cdots F) = 1.87$ Å and $R(H\cdots O) = 2.02$ Å, approximately $ES(H\cdots F)/ES(H\cdots O) \sim 0.8$, i.e., $(HF)_2$ will have a smaller ES.

CT is principally due to the $\pi \rightarrow \sigma^*$ interaction. The above δ suggests that, compared with H_2O, HF has less electrons on the proton and therefore has a larger MO coefficient on the proton for σ^* orbitals, which will contribute to a larger CT interaction. Of course, other factors such as the R dependence of CT can obscure the comparison, and this argument should be considered as just a conjecture.

The θ dependence of energy components is shown in Table XI. ES is most stable at around $\theta = 30°$. The dipole-dipole interaction would have preferred $\theta = 0$, hence an additional effect must be considered. As θ increases, CT stabilization increases but both EX and PL destabilize the complex. A

Table XI. Energy Components in kcal/mol for Linear $(HF)_2$ as Functions of θ[a]

	θ		
	30°	60°	90°
$\Delta\Delta E$	−0.2	−0.1	2.2
ΔES	−0.2	0.1	2.8
ΔEX	0.2	0.6	0.8
ΔPL	0.1	0.2	0.3
ΔCT	−0.2	−0.8	−1.5
ΔMIX	−0.1	−0.2	−0.2

[a] Other parameters from experiment: R = 2.79 Å and γ = 0 in Figure 3a. The energy is the difference from θ = 0.

Table XII. The Effect of Nonlinearity of the Hydrogen Bond Axis F- - -H-F on Energy Components in kcal/mol for Linear $(HF)_2$[a]

γ, deg	10	20	10	10
α, deg	0	0	90	180
$\Delta\Delta E$	−0.3	0.1	0.3	0.9
ΔES	−0.2	0.2	0.3	1.0
ΔEX	−0.2	−0.8	−0.2	−0.2
ΔPL	−0.0	−0.0	0.0	0.1
ΔCT	0.2	0.6	0.1	0.0
ΔMIX	0.0	0.1	0.0	0.0

[a] Geometrical parameters defined in Figure 3a. Other values are from experiment: R = 2.79 Å and θ = 60°. The energy is the difference from γ = 0.

delicate balance among all the components determines the optimum θ. Obviously this is the reason why the value θ is rather sensitive to the basis set employed and it is therefore difficult to obtain a reliable value. Though the angular dependence of ES is similar to that of $(H_2O)_2$, the fractional charge model used for $(H_2O)_2$ cannot be used here, since the fractional charge model in HF does not add anything to an argument based on dipoles. A model which takes higher multipoles into account has to be considered. A tempting explanation of this peculiar angular dependence of ES as well as that of EX is based on the electron distribution on the fluorine atom in a molecule.[41] The F atom has two π electrons in each direction but less than two σ electrons. Therefore the electron distribution is more dense (more negative) in the direction of the π orbitals than in the direction of the σ orbitals (the molecular axis). The proton thus prefers to approach the π side of electron density to increase ES. A balance between the large dipole-dipole interaction and this local effect would put the optimal angle for ES somewhere between 0 and 90°. This may also be interpreted as a balance between the dipole-dipole term and the contributions of higher multipoles. From an EX point of view, the proton would like to approach the least dense area, i.e., θ = 0, to avoid an overlap of electron clouds. CT's main contribution comes from the $\pi \rightarrow \sigma^*$ interaction. The linear

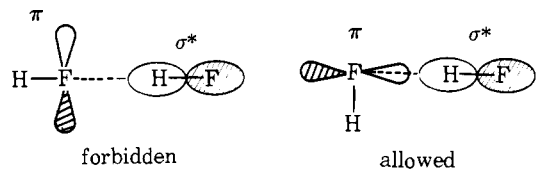

approach forbids such an interaction as is illustrated below. The perpendicular approach is the most desirable. This argument is similar to that presented for $(H_2O)_2$.

We now examine the effect of the nonlinearity of the $F_a \cdots F_c$ axis as defined by $\gamma = \angle H_d F_c F_a$ and the azimuthal angle α of rotation of $H_d F_c$ around the z axis (Figure 3a), where α = 0 corresponds to a trans and α = 180° to a cis structure. Table XII summarizes the results. The geometry with a small $\gamma >$ 0 with α = 0 (trans) is more stable than the linear geometry.[42] This stability is due to a gain in ES and a reduction in EX repulsion, partially negated by a loss in CT. The monotonic decrease in CT stabilization and monotonic reduction on EX can be easily understood in terms of the decreased overlap between orbitals as H_d swings away from the proton acceptor molecule. The variation of ES should be considered in conjunction with a large decrease in ES stabilization as the proton moves from the linear to a cis position (α = 180°). Apparently the proton H_d is feeling the repulsion of a positive charge on $H_b^{+\delta}$. By changing the deviation from cis through linear to trans one can reduce this repulsion and still can take full advantage of the attractive interaction with $F_a^{-\delta}$ at γ = 10° (cis). Beyond this ($\gamma >$ 10°, cis), H_d begins losing the interaction with $F_a^{-\delta}$ resulting in a loss in ES.

Table XIII. Energy Decomposition Analysis for H_3N-HF at Various Separation in kcal/mol (C_{3v} Approach)

	R, Å				
	2.60	2.68[a]	2.94	2.98	3.28
ΔE	−16.1	−16.3	−14.8	−14.4	−11.3
ES	−29.2	−25.6	−16.6	−15.6	−10.3
EX	21.1	16.0	5.8	5.0	1.5
PL	−2.3	−2.0	−1.1	−1.0	−0.5
CT	−5.1	−4.1	−2.5	−2.4	−1.8
MIX	−0.6	−0.7	−0.4	−0.4	−0.1

[a] Energy minimum obtained from a rational fraction fit.

C. Cyclic Dimer. Kollman and Allen[43] and Diercksen and Kraemer[44] optimized the geometry of a cyclic $(HF)_2$ (Figure 3b) and found R = 2.88 and 2.85 Å, respectively. Using Kollman and Allen's ϕ = 54.5° we have performed an energy decomposition, results of which are shown in the last column of Table X. For a comparable $R = r$(F-F), the cyclic dimer is less stable than the linear dimer in principle due to the 40% reduction in ES stabilization, which cannot be compensated for even by a 30% reduction in the EX repulsion. The misalignment of the dipoles on the cyclic dimer explains the ES loss. For the same R the cyclic form should have much less EX because the hydrogen bonding proton which is the major source of EX is not very close to the electron cloud of the F.

V. Complex H_3N-HF

H_3N-HF has the strongest hydrogen bond one can form by any combination of HF, H_2O, NH_3, and CH_4. This strong complex is another convenient system to study the origin of stability because it requires only one geometrical parameter $R = r$(N-F) to describe the most stable C_{3v} structure with a linear hydrogen bonding N- - -HF.[45] Table XIII shows the energy components as functions of R. At the calculated $R_e \sim$ 2.68 Å the complex is strongly ES supplemented by a substantial CT contribution. In order to analyze further the contributions to CT, its subcomponents $CT_{H_3N \rightarrow HF,\sigma}$, $CT_{H_3N \rightarrow HF,\pi}$, $CT_{H_3N \leftarrow HF,\sigma}$, and $CT_{H_3N \leftarrow HF,\pi}$ are calculated separately near R_e, as shown in Table XIV. The major portion (~90%) of CT is due to $H_3N \rightarrow HF,\sigma$, i.e., CT from the σ occupied orbitals of NH_3 to the vacant σ^* orbitals of HF, presumably from the highest occupied lone pair orbital to the lowest vacant σ^* orbital. The small back donation from HF to NH_3 is shared by $\sigma \rightarrow \sigma^*$ CT and CT from the HF π to the NH_3 π^* hyperconjugation orbital. This can be compared with $(H_2O)_2$, where the π contribution was negligibly small (section III).

Any deviation from the C_{3v} structure results in destabilization of the complex. Table XV lists the results for four such deformations with fixed r(N- - -H), as defined in Figure 4.

Table XIV. Further Decomposition of CT Energy in kcal/mol for H_3N-HF (C_{3v}) at R = 2.67 Å[a]

CT	$H_3N \rightarrow HF$	$H_3N \leftarrow HF$	Total
σ	−3.58	−0.34	−3.90
π	0.00	−0.21	−0.21
Total	−3.58	−0.55	−4.11

[a] Small coupling terms between σ and π or between $H_3N \rightarrow HF$ and $H_3N \leftarrow HF$ are not listed.

(a) Deviation of F from the C_{3v} Axis. A positive and negative $\alpha = \pi - \angle NHF$ put an HNHF in the cis and trans position, respectively. The destabilization is almost exclusively due to an increase in EX repulsion. A similar conclusion was drawn for the H_3N-BH_3 electron donor-acceptor (EDA) complex (Figure 4e) with $a = 0$ and $b \neq 0$, where EX was the principal destabilizing contribution.[12] In both cases one can attribute the EX increase to an increase in the overlap between the lone pair orbital of NH_3 and the electron cloud of the electron acceptor.

(b) Deviation of H of HF from the N-F Axis. $\beta > 0$ (<0) puts an HNFH in a cis (trans) position.

(c and d). Tilting of the NH_3, C_{3v} Axis from the NHF Axis by β or δ, Depending on the Direction of Deviation. For all cases (b), (c), and (d), the principal origin of destabilization is a loss in ES, partially compensated for by a decrease in EX. A similar situation was found for H_3N-BH_3 with $a \neq 0$ and $b = 0$.[12] Also, a similar competition between ES and EX is observed for $\gamma \neq 0$ in $(H_2O)_2$ (Table VI and Figure 1a) and $(HF)_2$ (Table XII and Figure 3a). This trend may be interpreted as follows. By misaligning the polarity of the electron donor with that of the electron acceptor, one suffers a loss in ES, but a smaller overlap between the donor lone pairs and/or π orbitals and the electron cloud of the electron acceptor reduces EX. The balance for most of the cases mentioned is such that ES destabilization is larger than the reduction in EX, making the "linear" structure the more stable. An exception is for a small $\gamma > 0$ for $(HF)_2$ where the EX reduction surpasses the ES destabilization, resulting in a complex whose equilibrium geometry is possibly slightly bent.

VI. Comparison between Hydrogen Bonded Complexes of HF, H_2O, NH_3, and CH_4

Detailed studies of energy decomposition for $(H_2O)_2$, $(HF)_2$, and H_3N-HF have been presented in the preceding sections. Additional calculations were carried out for other linear hydrogen bonded complexes between HF, H_2O, NH_3, and CH_4. For all the complexes in which H_2O was the proton acceptor and HYH_n was the proton donor, the atom O, the bond HY, and the bisector T of the H_2O bond angle are all assumed to be in the xz plane, as illustrated in Figure 1a. The nonhydrogen bonded protons of HYH_n were assumed to be oriented in such a manner as to minimize the proton-proton repulsion, as illustrated below. For each complex $R = r$(O-Y) and $\theta = \pi - \angle TOY$ are optimized. The R and θ dependencies of energy components are very similar to those of $(H_2O)_2$ given in Tables II and IV and will not be presented. For all the complexes in which NH_3 was the proton acceptor, the atom N and the bond HY were assumed to be collinear on the C_{3v} axis of NH_3, with the configuration of the nonhydrogen bonded protons of HYH_n assumed to be antiperiplanar, as illustrated below. The geometry was optimized for $R = r$(N-Y). The R dependence of energy components is similar to that for H_3N-HF and will not be presented.

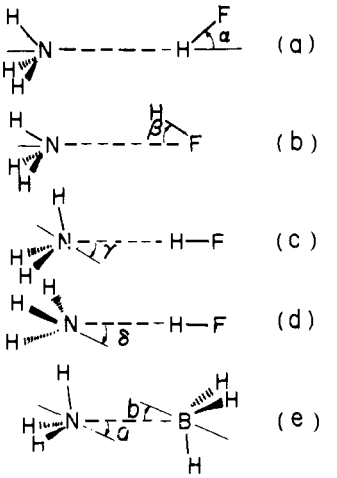

Figure 4. Four forms of deviation of H_3N-HF from the C_{3v} approach. r(N- - -H) is fixed at 1.753 Å. (e) is for H_3N-BH_3 where two deviation angles from the C_{3v} approach are defined.

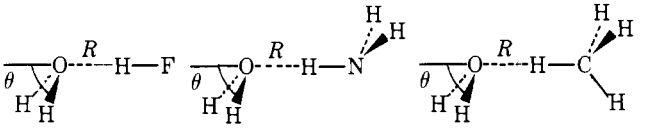

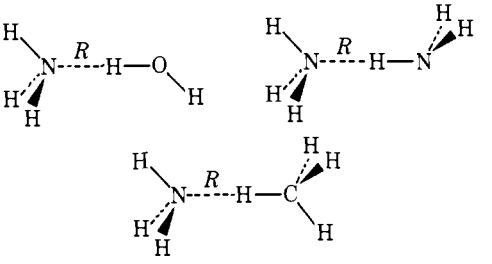

A. Comparison at Equilibrium Geometries. The energy components at calculated energy minimum for each compound are shown in Table XVI. The examination of the table reveals the following general trends. All the hydrogen bonds are strongly ES in nature, with a smaller but significant contribution of CT. The complex is the strongest at the left bottom

Table XV. Relative Energy Components in kcal/mol for H_3N-HF at r(N-H) = 1.753 Å for Various Deformations from the C_{3v} Approach[a]

	α				β		γ			δ
	10°	−10°	−20°	−30°	10°	−10°	10°	−10°	−20°	10°
$\Delta\Delta E$	0.2	0.2	1.0	2.4	0.9	0.9	0.4	0.4	1.4	0.4
ΔES	0.0	0.0	0.1	0.2	1.3	1.3	0.5	0.5	2.1	0.5
ΔEX	0.2	0.2	0.9	2.2	−0.8	−0.8	−0.2	−0.2	−0.7	−0.2
ΔPL	0.0	0.0	0.0	0.1	0.1	0.1	−0.0	−0.0	−0.1	−0.0
ΔCT	0.0	0.0	0.0	0.0	0.3	0.3	0.0	0.0	0.0	0.0
ΔMIX	−0.0	−0.0	−0.1	−0.1	−0.0	−0.0	0.0	0.0	0.1	0.0

[a] Energies relative to the C_{3v} structure. Deviations defined in Figure 4.

Table XVI. Comparison of Energy Components in kcal/mol between Various Linear Hydrogen Bonded Complexes

Proton acceptor	Proton donor HF	H_2O	H_3N	H_4C	HF	H_2O	H_3N	H_4C
	R, Å[a]				θ, deg			
HF	2.71				60[b]			
H_2O	2.62	2.88	3.22	3.80	6[c]	60[b]	60[c]	60[d]
H_3N	2.68	2.93	3.30	4.02	0[e]	0[d]	0[d]	0[d]
	ΔE				CT			
HF	−7.6				−3.2			
H_2O	−13.4	−7.8	−4.1	−1.1	−3.1	−2.4	−1.5	−0.9
H_3N	−16.3	−9.0	−4.1	−1.1	−4.1	−2.4	−1.3	−0.7
	ES				PL			
HF	−8.2				−0.4			
H_2O	−18.9	−10.5	−4.6	−0.5	−1.6	−0.6	−0.3	−0.1
H_3N	−25.6	−14.0	−5.7	−0.6	−2.0	−1.1	−0.6	−0.3
	EX				MIX			
HF	4.5				−0.3			
H_2O	10.5	6.2	2.5	0.5	−0.4	−0.5	−0.2	−0.0
H_3N	16.0	9.0	3.6	0.5	−0.7	−0.4	−0.2	−0.0

[a] $R = r(X\text{- - -}Y)$ is optimized by a rational fraction or a parabolic fit in this paper. [b] Experimental value. [c] Optimized by Kollman et al. (ref 35) with the present basis set. [d] Assumed. [e] Optimized.

corner (H_3N-HF) of the table and becomes progressively weaker as one moves from there to the right or to the top of the table. The equilibrium R depends sensitively on the proton donor but is not highly dependent on the proton acceptor.[2,35,46] The general trend of stability ΔE is controlled predominantly by ES, partly compensated by the opposite trend of EX and supplemented slightly by CT, PL, and MIX. This trend of ES cannot be understood if the dipole moment of the monomer (NH_3, 1.47 exptl (2.30 calcd with the 4-31G set); H_2O, 1.85 (2.60); HF, 1.83 (2.28) in D) is used as the measure of polarity. A simple-minded picture which can qualitatively explain the trend of ES in Table XVI is an interaction $\delta_X\delta_H/R_{HX}$ between the net charge δ_X on the proton acceptor atom X and the net charge δ_H on the hydrogen bonding proton.[47] Therefore one can conclude that the critical factor determining ES is not the overall molecular polarity but rather the local polarity at the hydrogen bonding region.

The net charge suggests that CH_4 may be a better proton acceptor than HF as far as ES is concerned. Unfortunately, it is expected that EX repulsion would be extremely large because of the overcrowding in a five-coordinated structure. Therefore, with an exception of $H_4C + H^+$ in which EX repulsion does not exist,[14] CH_4 would not function as a proton acceptor or an electron donor.

The trend of other components can also be understood qualitatively in terms of the net charge on the terminal atoms. EX prefers a contact between less electron rich groups. The preference for the proton acceptor, therefore, would decrease in the order F > O > N, and for the proton donor HCH_3 > HNH_2 > HOH > HF. For a given proton donor, as one changes the proton acceptor $H_3N \rightarrow H_2O \rightarrow$ HF, the EX reduction is so drastic that, although the ES stabilization is also reduced, R becomes comparable for all three complexes.

Since CT does not depend much on the proton acceptor and depends only weakly on the proton donor whereas ES shows a large change, the relative weight of CT in ΔE differs substantially within the series. For instance, in the weakest hydrogen bonds H_2O-HCH_3 and H_3N-HCH_3 CT is the largest contribution, making them "very weak CT-ES complexes". On the other hand, even if one takes into account the 4-31G's overestimation of ES, H_3N-HF should be called a "strong to intermediate ES complex". Other complexes distribute themselves between the two limits.

For a complex between NH_3 and H_2O, two possible modes of hydrogen bonding exist, H_3N-HOH and H_2O-HNH_2, of which the former is the more stable. Concordant with the above interpretation of the current trend, this difference is mainly due to ES, supplemented by CT and PL, and cancelled to a large extent by EX.

The rotational barrier around the hydrogen bond axis has been calculated for a few complexes. Table V shows for R = 2.98 Å, $\theta = 60°$ and $\gamma = 0$, the barrier of rotation of H_y (Figure 1a) is 2.3 kcal/mol, which is exclusively due to ES. Similar calculations for H_3N-HOH at 2.98 Å and H_3N-HNH_2 at 3.28 Å give no barrier to rotation, every component for the staggered conformation being identical within 0.01 kcal/mol to that for the eclipsed form. If the X- - -H-Y bond is replaced by a true single bond X′-Y′, H_2O-HOH looks like H_2N-OH, and H_3N-HOH and -HNH_2 look like H_3C-OH and -NH_2, respectively. The barrier for CH_3OH and CH_3NH_2 is small (~2 kcal/mol) and is due to EX.[48] Since EX is a short-range interaction, it would not contribute to the barriers of H_3N-HOH and -HNH_2, which have a "long X- - -H-Y single bond". The barrier for NH_2OH is large (the 4-31G value ~10 kcal/mol) and is principally due to ES, partially cancelled with EX and PL.[48a] Since ES is a long-range interaction, it is reasonable that a barrier for H_2O-HOH, a stretched version of NH_2OH, should exist and be controlled by ES.

B. Comparison at a Fixed R. In Table XVI energy components are compared at the equilibrium R for each compound. For a series of complexes with a given proton acceptor, as one travels a row of the table from the left to the right, the heavy atom distance $R = r(X\text{- - -}Y)$ increases as the complex becomes weaker and all individual components become smaller. This comparison does not, therefore, tell why a weaker complex for a given proton acceptor has a longer R. A better comparison for this purpose would be at the same intermolecular separation. Intermolecular separation can be defined as either the proton acceptor atom-proton distance $r(X\text{- - -}H)$ or the distance between the heavy atoms $r(X\text{- - -}Y)$. Another aspect is the choice of the value of the distance at which a comparison should be made. In order to reflect the importance of components in the stabilization, the distance should not be far away from the equilibrium of all the components. We arbitrarily chose $r(X\text{- - -}Y)$ = 2.98 Å and $r(X\text{- - -}H)$ = 2.024 Å. The energy components for linear complexes H_2O-HYH_n and

Table XVII. Relative Energy Components in kcal/mol for Various Linear Hydrogen Bonded Complexes at the Same Intermolecular Separation[a]

	Proton acceptor							
	H_2O with proton donor				H_3N with proton donor			
	HF	H_2O	H_3N	H_4C	HF	H_2O	H_3N	H_4C
				r(X- - -H) = 2.024 Å				
$\Delta\Delta E$	0	3.9	7.7	12.8	0	5.9	11.3	17.3
ΔES	0	2.6	4.8	7.7	0	3.8	7.0	10.2
ΔEX	0	1.5	2.8	4.9	0	1.6	3.5	6.3
ΔPL	0	0.3	0.3	0.4	0	0.1	0.2	0.2
ΔCT	0	−0.3	−0.1	0.0	0	0.4	0.4	0.2
ΔMIX	0	−0.2	−0.2	−0.2	0	0.0	0.2	0.5
				r(X- - -Y) = 2.98 Å				
$\Delta\Delta E$	(−11.2)	3.5	7.6	14.5	(−14.4)	5.5	11.3	19.5
ΔES	(−10.9)	2.0	3.4	4.7	(−15.6)	2.8	4.8	5.6
ΔEX	(2.3)	1.9	4.6	10.5	(5.0)	2.4	6.4	14.6
ΔPL	(−0.7)	0.0	0.0	0.0	(−1.0)	0.0	−0.0	−0.1
ΔCT	(−1.7)	−0.4	−0.3	−0.7	(−2.4)	0.3	−0.0	−1.5
ΔMIX	(−0.1)	−0.2	−0.3	−0.2	(−0.4)	0.0	0.1	0.8

[a] γ used is the value in Table XVI. Energies are relative to $(HF)_2$ and H_3N-HF, respectively, for which actual energy components are given in parentheses.

Table XVIII. Relative Energy and Its Components in kcal/mol for H_3N-HOZ Where Z = H, CH_3, NH_2, and F[a]

	Proton donor[b]			
	H_2O	CH_3OH	NH_2OH	FOH
Optimized R_e, Å	2.93	2.90	2.83	2.72
$\Delta\Delta E$	(−9.0)	−0.2	−1.0	−8.2
ΔES	(−14.0)	−0.8	−3.0	−12.9
ΔEX	(9.0)	1.3	3.7	9.1
ΔPL	(−1.1)	−0.3	−0.4	−1.3
ΔCT	(−2.4)	−0.4	−1.0	−2.5
ΔMIX	(−0.4)	−0.1	−0.3	−0.6
R, Å	2.98	2.98	2.98	2.98
$\Delta\Delta E$	(−8.9)	−0.2	−0.7	−6.7
ΔES	(−12.8)	0.0	0.2	−4.6
ΔEX	(7.5)	0.2	−0.3	−0.8
ΔPL	(−1.0)	−0.2	−0.2	−0.4
ΔCT	(−2.1)	−0.2	−0.3	−0.7
ΔMIX	(−0.4)	−0.1	−0.2	−0.3

[a] All energies are relative to H_3N-HOH, except for H_3N-HOH where the actual values are shown in parentheses. [b] Proton acceptor = NH_3.

H_3N-HYH_n, relative to H_2O-HF and H_3N-HF, respectively, are shown in Table XVII. The table indicates that for the fixed r(X- - -Y), as the proton donor changes as HF → H_2O → NH_3 → CH_4, the complex is destabilized mainly due to an increase in the EX repulsion, supplemented by a decrease in the ES attraction. The increase in EX repulsion with the change in the proton donor HF → CH_4 can be understood as the result of an increase in the electron cloud of the heavy atom Y and a decrease in the electron cloud of the proton as well as a decrease in the r(X- - -H), since r(H-Y) is largest for CH_4 and the smallest for HF. If r(X- - -H) is fixed, r(X- - -Y) would increase as one scans the proton donor from the left to the right. For the fixed r(X- - -H), EX is already partly relaxed compared to the fixed r(X- - -Y), and the smaller stability is mainly due to the smaller ES stabilization, supplemented by the larger EX repulsion. It is not obvious whether one should compare a series of complexes at R_e or the fixed r(X- - -H) or the fixed r(X- - -Y). One can say, however, that at the fixed r(X- - -Y) a weaker complex feels much stronger EX repulsion than a stronger complex. By making r(X- - -Y) larger, the weak complex releases the EX repulsion accompanied by a loss in ES. At the equilibrium geometry, the difference in the stability between a weak and a strong complex for a given proton acceptor is determined principally by ES.

VII. Substituent Effects in Hydrogen Bonding

Extensive MO studies of substituent effects in hydrogen bonding have been carried out by Del Bene on CH_3HO-HOH, H_2O-HOR, H_3N-HOR, and H_2CO-HOR where R = H, CH_3, NH_2, OH, and F.[49] We expect that energy decomposition analyses of hydrogen bonding complexes, coupled with comparisons to other types of complexes (EDA complexes and protonation complexes), should aid in determining the origin of the hydrogen bond. The results of two series of calculations, one on H_3N-HOZ, where Z = H, CH_3, NH_2, or F, and the other on H_3N- and CH_3H_2N-HOH will be presented.

A. Substituent Effect on the Proton Donor HOZ in H_3N-HOZ. A series of complexes between the proton acceptor H_3N and proton donors HOZ where Z = H, CH_3, NH_2, and F was examined. In order to ensure maximum stability, the complex was assumed to have a collinear N-HO on the C_{3v} axis of NH_3, and the nonhydrogen bonded group was assumed to be in the antiperiplanar position, as shown below. The experimental OH distances were used (section II), which are all

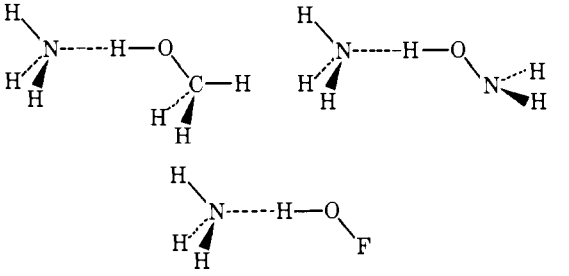

around 0.96-0.97 Å. The energy components at the optimized $R = r$(N-O) for each complex and at R = 2.98 Å are shown in Table XVIII. At the same N-O distance, the stability of the complex as a function of the Z substituent increases in the order H < CH_3 < NH_2 < F. The origin of the stabilization is not clear and uniform. Changes in CT, PL, and EX all seem to make essential contributions for Z = CH_3 and NH_2, and for Z = F, the increase in ES stabilization is obviously the most important source of the substituent effect. If one examines the complexes at their equilibrium separations (larger for weaker

Table XIX. A Comparison of Interaction Energy Components and *N*-Methyl Substituent Effects between Various Complexes at Equilibrium Geometry (kcal/mol)

	Complex				
	H_3N-HOH	H_3N-ClF[a]	H_3N-BH_3[b]	H_3N-H^+[c]	H_3N-Li^+
R_e, Å[d]	2.93	2.717	1.705	1.02	2.01
ΔE	−9.0	−8.2	−44.7	−221.9	−50.8
ES	−14.0	−11.2	−92.9	−99.8	−53.6
EX	9.0	7.4	86.9	0.0	11.8
PL	−1.1	−1.1	−17.2	−27.4	−6.4
CT	−2.4	−3.6	−27.1	−88.3	−2.7
MIX	−0.4	0.2	5.6	−6.5	0.0
	Methyl Substituent Effect[e]				
$\Delta\Delta E$	0.2	0.3	−0.8	−8.5	2.0
ΔES	0.3	0.3	−1.2	3.3	4.2
ΔEX	0.2	0.5	4.4	0.0	0.4
ΔPL	−0.1	0.0	−5.0	−12.8	−2.6
ΔCT	−0.2	−0.6	−1.4	−3.4	−0.2
ΔMIX	−0.1	−0.0	2.4	4.4	0.2

[a] Reference 13. [b] Reference 12. [c] Reference 14. [d] The equilibrium intermolecular separation. The distance between N and the closest atom (Cl, B, H^+), except in H_3N-HOH, where R_e is the N-O distance (r(N-H) = 1.974 Å). [e] The difference between the CH_3H_2N complex and the H_3N complex. A negative number indicates that the CH_3H_2N complex is more stable, and vice versa.

complexes and smaller for stronger complexes), an increase in ES compensated largely by an increase in EX repulsion appears to be the critical factor, though the role of PL and CT is not negligible.

B. Substituent Effect on the Proton Acceptor NH_3 in H_3N-HOH. A single calculation has been performed for the CH_3H_2N-HOH complex at the calculated equilibrium geometry of H_3N-HOH (section VI and Table XVI), i.e., r(N- - -O) = 2.93 Å and r(N- - -H) = 1.974 Å with a collinear N- - -H-O on the C_{3v} axis of NH_3. The interaction energy components and their differences between CH_3H_2N-HOH and H_3N-HOH are shown in the second column of Table XIX. Also shown are the energy components and their methyl substituent effects for the other complexes we have studied in previous papers[12-14] in which H_3N is the electron donor: H_3N-ClF (an intermediate EDA complex), H_3N-BH_3 (a strong EDA complex), H_3N-H^+ (a protonation complex), and H_3N-Li^+ (lithium ion complex, which is to be discussed in section VIII).

The overall substituent effect is small for H_3N-HOH. $[\Delta E(CH_3H_2N \text{ complex}) - \Delta E(H_3N \text{ complex})]/\Delta E(H_3N \text{ complex}) = \Delta\Delta E/\Delta E(H_3N \text{ complex})$ is only 2%. This case can be compared with the other complexes where the calculated substituent effect is large (H_3N-ClF, H_3N-H^+, and H_3N-Li^+, all 4%) or small (H_3N-BH_3, 2%). The small overall substituent effect for H_3N-HOH is due to a cancellation between (ΔES + ΔEX) > 0 and ΔCT < 0. Though the magnitude of the overall substituent effect is somewhat different, the trend of the components of the substituent effect for H_3N-HOH is rather similar to that for H_3N-ClF in that ΔES > 0, ΔEX > 0, and ΔCT < 0 and all are similar in magnitude. Interestingly, both are complexes of intermediate strength with a large intermolecular separation, though one is hydrogen bonded and the other is nonhydrogen bonded. In the same sense, the trend of component substituent effects for H_3N-BH_3 is similar to that of H_3N-H^+, both series having a large ΔPL contribution. Both are strong complexes with a short intermolecular distance. A critical difference between the two

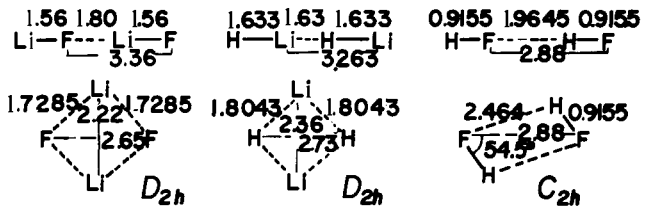

Figure 5. Geometries of $(LiF)_2$, $(LiH)_2$, and $(HF)_2$ compared in Table XX.

complexes, as was discussed previously,[12] is that EX does not exist in the protonated complex.

It is interesting to note that in all the complexes in Table XIX, the component methyl substituent effect is ΔES > 0 (except in H_3N-BH_3), ΔEX > 0 (except in H_3N-H^+ where EX does not exist), ΔPL < 0, and ΔCT < 0. Namely, the methyl group on the N atom of NH_3 increases the PL and CT stabilization, while it destabilizes the complex by reducing the ES stabilization and increasing the EX repulsion. The diversity of the overall substituent effect $\Delta\Delta E$ is the result of different cancellation between opposing components. More discussions on the substituent effect will be given in section IX.

VIII. Comparison with Lithium Complexes

A. $(LiF)_2$, $(LiH)_2$, and $(HF)_2$. In order to shed light on the question of whether the stability of hydrogen bonds is unique and, if so, why, Kollman et al.[50] paid attention to complexes involving "Li bonding". They carried out calculations for complexes of HF, LiF, Li_2, and LiH. The MO theory predicts the correct, cyclic structure for $(LiF)_2$ as well as the correct, linear structure for $(HF)_2$. A comparison of the energy decomposition analysis among linear and cyclic structures of $(LiF)_2$ and $(HF)_2$ should be very informative as to the origin of the different geometric preference of the two dimers. $(LiH)_2$ also serves as a guide of comparison.

The calculations for $(LiF)_2$ and $(LiH)_2$ were carried out at the optimized linear and cyclic geometries of Baskin et al.,[50c] as shown in Figure 5. One should note first that the cyclic form of $(LiF)_2$ and $(LiH)_2$ both have a D_{2h} symmetry, i.e., the intramolecular and intermolecular Li-F(H) distances are identical, whereas $(HF)_2$ has a cyclic dimer of C_{2h} symmetry. The energy decomposition for cyclic $(LiF)_2$ and $(LiH)_2$ was carried out by using the stretched Li-F and Li-H, respectively, as the reference monomer. Therefore, the energy DEF required for stretching the monomers has to be taken into account if one wants to compare a cyclic complex with a linear one. The results of the energy decomposition are shown in Table XX, where the results for $(HF)_2$ from Table X are also included.

A comparison of the linear form between $(LiF)_2$ and $(HF)_2$ reveals that the former is a much stronger complex with most (~81%) of the attractive components coming from ES, deserving to be called "a strong ES complex". $(HF)_2$ is a much weaker complex with ES contributing ~68% and CT ~26% of the attraction and is to be called "an intermediate ES-CT or ES > CT complex". The larger ES in $(LiF)_2$ is partially due to the larger polarity of the monomer (4-31G atomic population and calculated dipole moment: $Li^{+0.73}$-$F^{-0.73}$, 6 D, vs. $H^{+0.48}$-$F^{-0.48}$, 2.3 D) and partly to the smaller intermolecular separation (r(Li- - -F) = 1.80 Å vs. r(H- - -F) = 1.96 Å). The linear $(LiH)_2$ is "a strong ES > PL,CT complex". The polarity is quite large ($Li^{+0.27}$-$H^{-0.27}$, 6 D) and the intermolecular separation r(Li- - -H) = 1.63 Å is extremely small. It is noted for this complex that even at this small separation EX repulsion is not overwhelmingly large due to the small size of electron clouds for both Li and H.

The cyclic $(LiF)_2$ is apparently much more stable than the linear form, because of an extremely favored ES supplemented

Table XX. Comparison of Energy Components in kcal/mol for Lithium and Hydrogen Bonded Complexes

	$(LiF)_2$			$(LiH)_2$			$(HF)_2$		
	Linear $C_{\infty v}$	Cyclic D_{2h}	Δ^a	Linear $C_{\infty v}$	Cyclic D_{2h}	Δ^a	Linear $C_{\infty v}$	Cyclic C_{2h}	Δ^a
ΔE	−44.7	−75.4	30.7	−24.8	−44.6	19.8	−7.6	−5.6	−2.0
DEF[b]		2 × 4.5	−9.1		2 × 1.6	−3.3			
ES	−44.5	−98.1	53.7	−33.8	−79.7	45.9	−8.2	−3.9	−4.3
EX	10.6	40.2	−29.6	17.3	51.7	−34.5	4.5	0.7	3.8
PL	−0.3	−8.6	8.3	−11.4	−13.0	1.7	−0.4	−0.5	0.1
CT	−6.1	−14.6	8.5	−8.7	−55.0	46.2	−3.2	−3.0	−0.2
MIX	−4.4	−3.3	−1.1	11.9	48.1	−36.2	−0.3	−0.1	−0.2

[a] The difference between the linear and the cyclic structure. [b] The energy required to stretch the monomer to the bond length in the cyclic dimer.

in a small portion by CT and PL. The gain in ES is so large (~55 kcal/mol) that one can form a stable cyclic form by overcoming the overcrowding of electrons (i.e., an increase in EX repulsion by ~30 kcal/mol) and the energy loss required to stretch two LiF molecules (~9 kcal/mol). A very similar situation is also observed for the cyclic structure of $(LiH)_2$. The fact that the energy loss is very small in stretching the bond to a large separation (1.7–1.8 Å) for both LiH and LiF favors the cyclization process. On the other hand, for $(HF)_2$ ES is not large enough to accommodate the stretching of bonds necessary in forming a D_{2h} complex. The fact the HF has a rather short bond distance and requires a larger energy than LiF to stretch to a comfortable distance (1.7–1.8 Å) also disfavors the cyclization.

Concluding the comparison, one may say $(LiF)_2$ and $(LiH)_2$ are complexes which are very different from the hydrogen bonded $(HF)_2$. The difference can be seen in the total interaction energy, components, and the preferred geometries.

B. Energy Components and Methyl Substituent Effects in H_3N-Li^+. In section VIIB we examined the *N*-methyl substituent effects in the H_3N-HOH hydrogen bonded complex and compared the calculated energy components for various intermolecular complexes in which NH_3 and its methyl derivatives serve as an electron donor.[12-14] The most profound methyl substituent effect has been observed for the proton affinity. The energy component analysis reveals that the protonated complex is a strong ES-CT > PL complex. The trend of the methyl substituent effect (with successive methyl substitution the proton affinity increases, which is opposite to what is expected from a simple electrostatic model) was attributed to the polarization effect (Table XIX).

For a better understanding of the proton affinity and the difference in behavior between H^+ and Li^+, we were interested in comparing the energy components and the origin of methyl substituent effects between the proton affinity and the lithium ion affinity. Calculations were carried out for H_3N-Li^+ (C_{3v}) as a function of $r(N\text{-}Li^+)$. A parabolic fit for ΔE = −48.1, −50.8, and −45.8 kcal/mol at 1.8, 2.0, and 2.3 Å gave the optimized $R = r(N\text{-}Li^+)$ = 2.01 Å. The energy components for H_3N-Li^+ and for the methyl substituent effect, the difference between CH_3H_2N-Li^+, and H_3N-Li^+, are shown in the last column of Table XIX.

H_3N-Li^+, which has an optimum R_e = 2.01 Å, is a strong complex, but only one fourth as strong as H_3N-H^+ where $R_e = r_e(N\text{-}H^+)$ = 1.02 Å. The analysis indicates that the existence of the EX repulsion keeps Li^+ further away from NH_3 than H^+ in which EX does not exist. Since $r_e(N\text{-}Li^+)$ is twice as large as $r_e(N\text{-}H^+)$, in the Li^+ complex only the long-range interaction ES contributes significantly to the attraction. It is "a strong ES complex". The predicted *N*-methyl substituent effect (the methyl group reduces the lithium ion affinity) is opposite to what is predicted and observed for the proton affinity. The origin of this trend and difference with the proton affinity can be clearly understood by the component analysis. For the H^+ complex, PL was the controlling term. Methyl groups made ammonia more polarizable, i.e., they increase the H^+-induced multipole interaction. For the Li^+ complex, the role of the short-range PL in the methyl substituent effect is less important, because the intermolecular separation is twice as large as for the H^+ complex. The long-range ES, which was the largest contributor to the proton affinity itself, is also the commanding component for the methyl substituent effect. Obviously the difference in the EX repulsion between Li^+ and H^+ makes a large difference in the intermolecular separation and the nature of the binding.

IX. Discussions and Conclusions

In this last section of the paper we summarize the results of the present paper and our previous papers and present concluding discussions on five questions concerning the origin of hydrogen bonding.

A. What Are the Essential Energy Components in Hydrogen Bonding? Results rendering the answer to this question have been presented in sections III, IV, and V for individual systems, $(H_2O)_2$, $(HF)_2$, and H_3N-HF, respectively. We also presented results in section VI for a series of dimeric complexes between HF, H_2O, NH_3, and CH_4.

The energy components are strongly distance dependent. At a relatively small separation, ES, CT, and PL can all be important attractive components, competing against a large EX repulsion. At longer distances for the same complex the short-range attractions CT and PL are usually unimportant and ES is the only important attraction. In answering the above question, we restrict ourselves to the equilibrium geometry, because this is the only geometry experiments can probe.

It is also noted that the importance of an individual component depends on the kind of hydrogen bonding being considered. In ionic hydrogen bonds, the intermolecular separation is small and the hydrogen bond energy is extremely large. The example of the H_3N-H^+ complex has been shown in Table XIX. The H_2O-H^+ complex has the following components: ΔE = −182, ES = −79, PL = −29, CT = −71, and MIX = −3 kcal/mol. These protonation complexes are very strong ES-CT complexes. The $[FHP]^-$ complex, which we have examined previously,[51] has the following interaction energy components: path A, ΔE = −48, ES = −85, EX = 78, PL = −6, CT = −26, MIX = −9, ΔE_a = −15 kcal/mol; path B, ΔE = −84, ES = −91, EX = 65, PL = −7, CT = −35, MIX = −16, ΔE_a = 22 kcal/mol. In path A HF at its equilibrium geometry forms a complex with F^- to gain the stabilization ΔE and then relaxes its r(HF) to the most stable complex geometry gaining an extra stabilization ΔE_a. In path B, HF is at first stretched to the r_e(H- - -F) of the complex (hence $\Delta E_a > 0$),

then the complex is formed. In either case, this complex is a very strong ES > CT complex.

What we are more concerned with here is not such strong ionic complexes but "normal" hydrogen bonded complexes in which the proton acceptor atom is a neutral electronegative atom such as N, O, and F, and the proton donor group is a neutral polar bond such as F-H, O-H, and N-H. The C-H bond may also be included. As was discussed in section VIA and Table XVI, *all these hydrogen bonds are strongly ES in nature, with a small but significant contribution of CT.* This statement seems to apply not only to the total interaction energy but also to the individual MO energies in the complex (Table III). The strength of proton donors decreases in the order F-**H** > O-H > N-H > C-H, and the strength of proton acceptors decreases in the order N > O > F. Since CT does not change its magnitude from complex to complex as much as ES, the relative importance of CT varies substantially. The N- - -H-F bond is the strongest and is essentially ES in nature, the contribution of CT not being essential for binding. The X- - -H-C complex is a CT-ES complex, both components making an essential contribution to this very weak binding. Other complexes of the above proton donors and acceptors distribute themselves somewhere between the two extremes. Qualitatively ES appears to be mainly controlled by the local interaction between the net charges on the proton acceptor atom X and the net charge on the hydrogen bonding proton H or the dipole moment on the bond H-Y. CT will be discussed separately in the next subsection. PL is always the smallest attractive component and is not essential for binding; however, it does play an important role in some substituent effects on the interaction energy (question D) and in the charge redistribution (question B).

B. What Is the Role of Charge Transfer and What Determines the Electron Redistribution? As was discussed above, *CT is usually the second largest attraction in hydrogen bonding. It plays a relatively minor role in a strong, more ES hydrogen bond such as N- - -H-F but is essential for stabilization of weaker hydrogen bonds.* The principal CT contribution comes from the proton acceptor → proton donor charge transfer through the σ-type interaction (Tables I and XIV). Neither the proton donor → proton acceptor back-donation nor the charge transfer through π-type interaction is usually very significant (<15%). This is in a rather marked contrast with the strong back-donation found in the EDA complex OC-BH_3, where about one-third of CT stabilization comes from the OC ← BH_3 π back-donation.

The charge redistribution decomposition in hydrogen bonding has been discussed in previous papers; i.e., $(H_2O)_2$, H_2CO-HOH, and C_3H_2CO-HOH in Figures 2, 3, and 7, respectively, of ref 9 and for ClF-HF in Figure 4 of ref 13. There are also results for H_3N-H^+ in Figure 2 of ref 14. One should also refer to the charge decomposition analysis for varieties of EDA complexes in ref 13. An examination of these figures reveals general features of charge redistribution in "normal" hydrogen bonding. (a) *The electron density on and in the vicinity of the hydrogen bonding proton decreases due to EX and PL.* (b) *The electron density buildup on the proton acceptor side of the X- - -H interaction region is principally due to CT and PL.* (c) *The charge redistribution in the noninteracting part of the proton donor and the proton acceptor follows a typical bond charge alternation pattern*

$$\cdots R_2 \overset{+\delta' \; -\delta'}{\text{———}} R_1 \overset{+\delta \; -\delta}{\text{———}} X \cdots H \overset{+\delta \; -\delta}{\text{———}} Y \overset{+\delta' \; -\delta'}{\text{———}} R_1' \overset{+\delta'' \; -\delta''}{\text{———}} R_2' \cdots$$

which is dictated by PL. (d) *PL is the largest contributor to the charge redistribution,* despite the fact that PL is the smallest attractive energy component. (e) Because of (d), in many hydrogen bonded complexes the total density difference plot $\Delta\rho(\mathbf{r})$ looks qualitatively similar to the PL density plot $\rho_{PL}(r)$.

C. What Are Factors Determining the Geometrical Parameters of Hydrogen Bonded Complexes? By the geometrical parameters we mean in particular the intermolecular distance r(X- - -Y) or r(X- - -H), the hydrogen bond directionality, and the linearity of the X- - -H-Y hydrogen bond.

(i) **The Hydrogen Bond Distance.** The intermolecular distance is of course determined by the balance between the sum of the attractive force components ∂(ES + CT + PL + MIX)/∂R and the repulsive force ∂EX/∂R. The magnitude of the distance dependence of energy components plays the essential role.[12,51] For protonation complexes, EX does not exist; at the shorter distance the proton-proton acceptor nuclear repulsion included in ES dominates this component and ∂ES/∂R balances with ∂(CT + PL + MIX)/∂R. ∂ES/∂R becomes repulsive only when the proton penetrates through the electron cloud of X to have an unscreened interaction with the X nucleus. Because of this and the strong ion-polar molecule ES attraction, R_e is very small. The strong ES attraction makes R_e small also in other ionic hydrogen bonded complexes.

Turning to the "normal" hydrogen bond, one noticed in Table XVI that the equilibrium r(X- - -Y) depends sensitively on the proton donor but is not strongly dependent on the proton donor.[2,35,46] From the analysis in section VI, one can say that *for a given proton donor, as the proton acceptor X changes N → O → F, the reduction in EX is so drastic that, although the ES stabilization is also reduced, R becomes comparable for all three complexes.*

For a given proton acceptor, as the proton donor changes FH → OH → NH → CH, the complex becomes weaker and r_e(X- - -Y) increases. The differences in the energy components between these complexes are the direct consequence of differences in r_e(X- - -Y). A better comparison in search of the difference in r_e(X- - -Y) is to compare the complexes at a fixed r(X- - -Y), as was actually shown in Table XVII. *At a fixed r(X- - -Y) for a given proton-acceptor X, the weaker complex (e.g., the proton donor HY = HC) feels a much larger EX repulsion than the stronger complex (e.g., HY = HF) probably due to a larger electron density on the proton. By making r(X- - -Y) longer, the weaker complex relaxes the EX repulsion at the expense of a smaller loss in ES.*

(ii) The hy**drogen bond directionality,** by which we mean the direction of approach the proton donor Y-H to X in relation to the bond(s) X has. For $(H_2O)_2$ $\theta \sim 35°$ is found (Table IV, section IIIB), where θ is the angle between the hydrogen bond axis O- - -H-O and the bisector T of the proton acceptor HOH angle (Figure 1a). For $(HF)_2$, the calculated minimum is $\theta \sim 30°$ (Table XI, section IIIB) where θ is the angle between the hydrogen bond axes F- - -H-F and the proton acceptor HF (Figure 2a). For H_3N-HF any tilting (γ and δ in Figures 4c and 4d) of the NH_3 C_{3v} axis from the N- - -N-F axis destabilizes the complex (Table XV, section V).

In the three cases studied in detail, *the minimum in the total interaction energy is depicted almost exactly by ES.* Yet for both $(H_2O)_2$ and $(HF)_2$, ES is not the component which shows the largest angular dependence. The large increase in CT stabilization as θ increases cancels almost completely with the destabilization due to EX and PL. Any failure of complete cancellation could shift the minimum from the one predicted by ES, but this has not happened. For H_3N-HF, tilting decreases the EX repulsion, but a large decrease in ES prevents it from occurring.

The dipole-dipole model fails to reproduce the geometry predicted by ES. Higher order multipoles have to be taken into account, if the expansion is used. Instead, we have shown in section IIIB that a simple fractional charge model for H_2O ($+\delta$ on H and -2δ on O) can qualitatively reproduce the geometry

of $(H_2O)_2$. For HF, the nonspherical charge distribution around the fluorine atom has been used in section IVB to qualitatively explain the θ dependence for $(HF)_2$. In earlier studies[5] on H_2CO-HOH and $(H_2O)_2$ we have proposed that the directionality is dictated by the direction of the "lone pair" electrons on the proton acceptor. The fact that the fractional point charge model can explain the geometry and the lack of energy minimum in CT angular dependence near the ΔE minimum suggests that such an interpretation is too naive.

(iii) **The linearity of the hydrogen bond,** which refers to the fact that the hydrogen bond X- - -H-Y is collinear or nearly so in most cases. *The general preference of linear hydrogen bonding and possible slight deviations from it seem to be controlled mainly by changes in ES and EX.* A deviation of proton from the hydrogen bond axis with a fixed r(X- - -Y) reduces the EX repulsion. For a small $\gamma > 0$ (Figure 3a) in $(HF)_2$, this reduction combined with a loss in CT and a gain in ES puts the hydrogen bond slightly nonlinear, as is seen in Table XII. For a small $\gamma > 0$ (Figure 1a) in $(H_2O)_2$, a reduction in the EX repulsion is almost completely cancelled by a decrease in ES and CT, making the potential very flat, and for $\gamma < 0$, ES actually destabilizes the complex. For H_3N-HF, the ES reduction is larger than the EX reduction, forcing the bond to remain linear. A deviation of the atom Y from the hydrogen bond axis with a fixed r(X- - -H) is not favored because it accompanies an increase in the EX repulsion, as was discussed for $(H_2O)_2$ in section IIIB and for $(HF)_2$ in Table XV for $\alpha \neq 0$.

The cyclic and bifurcated structures are less favorable than the linear hydrogen bond structure because of a reduction in ES. As was discussed in Table IX for $(H_2O)_2$ and in Table X for $(HF)_2$, a substantial (25-40%) loss in the ES stabilization cannot be compensated by an even more substantial (30-60%) reduction in the EX repulsion.

D. Substituent Effects in Hydrogen Bonding and Comparison with Those in Proton Affinity and EDA Interaction. Substituent effects in hydrogen bonding have been examined in section VII and compared with the effects in other intermolecular interactions such as proton affinity, lithium ion affinity, and EDA interaction. A general conclusion is that *the sign and relative magnitude* $[\Delta E_{substituted} - \Delta E_{unsubstituted}]/\Delta E_{substituted}$ *of the overall substitution effects as well as the sign, magnitude, and importance of individual energy components depend not only on the reactants but also on the process involved.* A clear example presented in Table XIX and discussed in detail in section VIIB for varieties of complexes in which NH_3 and NH_2CH_3 are the electron donors indicates that the sign could be minus (CH_3 stabilizes the complex) or plus, the magnitude could be 2 to 4%, and the controlling components could be either PL alone or PL and ES or PL and EX or CT and EX + ES. Results for these complexes can be summarized as shown below in the following format: the complex; the interaction energy ΔE of the unsubstituted complex in kcal/mol; its origin(s); the sign and relative magnitude of N-methyl substituent effect; its origins in the decreasing order of importance and their signs.

RH_2N-H^+; −220; ES-CT > PL; −4%; ΔPL < 0

RH_2N-Li^+; −50; ES; +4%; ΔES > 0, ΔPL < 0

RH_2N-BH_3; −45; ES > CT; −2%; ΔPL < 0, ΔEX > 0

RH_2N-ClF; −8; ES > CT; +4%; ΔCT < 0, ΔEX > 0, ΔES > 0

RH_2N-HOH; −9; ES; +2%; ΔES > 0, ΔEX > 0, ΔCT < 0

Despite the varieties of the controlling components above, the signs of the individual components seem to be universal, with a few exceptions, to all the complexes: ΔES > 0, ΔEX > 0, ΔPL < 0, and ΔCT < 0.

The proton acceptor methyl substituent effect for H_3N-HOH above can be compared with the proton donor substituent effect:

H_3N-HOR; −9; ES; −2%; ΔEX > 0, ΔCT < 0, ΔPL < 0

Though the overall substituent effects in the two cases are of opposite sign and the predominant components are partially different, individual components have the same sign in both donor and acceptor effects.

E. What Makes Hydrogen Bonding Unique? A better question to begin with may be: "Is hydrogen bonding unique?" An approach to this question is to examine energy components between hydrogen bonded and nonhydrogen bonded forms of the same complex. This has been been performed for ClF-HF and FCl-HF at their calculated equilibrium geometries.[13]

ClF-HF: ΔE = −4.7, ES = −4.8, EX = 2.9, PL = −0.7, CT = −2.1, MIX = 0.0 kcal/mol

FCl-FH: ΔE = −3.4, ES = −3.6, EX = 1.8, PL = −0.2, CT = −1.4, MIX = 0.1 kcal/mol

or with the 4-31G** basis set at the 4-31G optimized geometries;

ClF-HF: ΔE = −2.5, ES = −2.7, EX = 3.0, PL = −0.8, CT = −2.3, MIX = 0.2 kcal/mol

FCl-FH: ΔE = −3.2, ES = −3.0, EX = 1.7, PL = 0.2, CT = −1.9, MIX = 0.1 kcal/mol

Surprisingly the energy components are rather similar between the two forms! Trying to be discriminatory, one finds that the role of ES is more important in ClF-HF than in FCl-HF and that the largest difference in the energy component in the 4-31G** set comes from EX. Since r_e(F- - -F) = 2.78 Å and r_e(Cl- - -F) = 2.73 Å are comparable, one may be tempted to say that the proton in the hydrogen bonded complex is unique in that it is buried deep in the interaction region. To examine whether this is a common trend, we compare various "normal" hydrogen bonds in Table XVI with some EDA complexes we have studied.[13]

H_3N-BH_3: R_e = 1.70 Å, ΔE = −44, ES = −93, EX = 87, PL = −17, CT = −2.7, MIX = 6 kcal/mol

H_3N-ClF: R_e = 2.72 Å, ΔE = −8, ES = −11, EX = 7 PL = −1, CT = −4, MIX = 0 kcal/mol

H_3N-ClF, which has ΔE comparable with $(HF)_2$, has a larger EX than the latter. No clear picture emerges from this kind of comparison. We also found in section VIIB that the trend of individual components of the N-methyl substituent effect for the hydrogen bonded complex H_3N-HOH is very similar to the nonhydrogen bonded complex H_3N-ClF.

A clue to the uniqueness comes from a comparison of energy components between hydrogen bonded complex $(HF)_2$ and lithium bonded complexes $(LiF)_2$ and $(LiH)_2$. As was discussed in detail in Table XX and section VIII, the two kinds of complexes are very different in nature, i.e., in the total interaction energy, its components, and preferred geometries. Discussions in section VIII suggest that *the uniqueness of "normal" hydrogen bonding lies in the basic fact that it always involves a moderately polar, short, and strong H-Y bond as the proton donor.* Because the polarity is moderate, the ES attraction is not so strong. The EX repulsion enhanced by the short H-Y bond prevents the hydrogen bonding proton from approaching closely to the proton acceptor. Since the H-Y bond is rather strong, stretching it to obtain more degrees of freedom for stronger bonding costs too much energy to be re-

covered. Because of these serious restrictions, *the "normal" hydrogen bond is always an intermediate to weak interaction* with linear bonding and appropriate directionality.

In EDA complexes, there is no intervening proton, and a strong electron acceptor and a donor can come to a close contact as in $OC-BH_3$ and H_3N-BH_3. In lithium bonding, one can stretch the monomer bond length without loss of much energy to allow more flexibility in bonding, allowing such structures as the D_{2h} cyclic complex. The above uniqueness of "normal" hydrogen bonding does not apply to "strong" hydrogen bonding involving cations and anions. Here the ionic environment gives rise to a large ES, which in turn allows more flexibility in monomer geometry changes and in the distance of approach. The situation in strong hydrogen bonds is therefore similar to strong EDA complexes and lithium bonds.

Acknowledgment. The authors are grateful to Drs. K. Kitaura, S. Yamabe, and A. Komornicki and Mr. J. O. Noell for helpful discussions and also to Drs. P. A. Kollman and L. C. Allen for comments on the manuscript and their preprints. The research is in part supported by the National Science Foundation and by the Center for Naval Analyses of the University of Rochester. H.U. is on leave from Kitasato University, Tokyo, Japan.

Appendix

In the method of Kitaura-Morokuma,[6,12] the Hartree-Fock **F** and the overlap **S** matrix are constructed based on the molecular orbitals ϕ_i^{A0} and ϕ_i^{B0} of isolated molecules, A and B.

$$\mathbf{D}(E) \equiv \mathbf{F} - \mathbf{S}E = 0 \qquad \text{(A-1)}$$

The matrix **D** is blocked for occupied MO's of A (A_{occ}), vacant MO's of A (A_{vac}), occupied MO's of B (B_{occ}), and vacant MO's of B (B_{vac}). If one carries out an SCF iterative calculation retaining only the diagonal blocks and the blocks connecting A_{occ} and B_{vac} ($A_{occ} \rightarrow B_{vac}$) and $B_{occ} \rightarrow A_{vac}$, as illustrated in a, and putting all the other blocks to zero, one obtains the energy $E_6 = E_0 + ESX + CT$ which includes the energy of the monomer (E_0), the electrostatic interaction with the intermolecular exchange integral contribution (ESX), and the charge transfer interaction (CT). If only the diagonal blocks are retained, as in b, the energy $E_5 = E_0 + ESX$ is obtained. The difference $E_6 - E_5$ gives the CT energy. If one includes the diagonal blocks and $A_{occ} \rightarrow B_{vac}$ block, as in c, one obtains $E_0 + ESX + CT_{A\rightarrow B}$, where $CT_{A\rightarrow B}$ is the energy due to the A→B charge transfer. Extending the method further, if one includes the matrix elements of $\mathbf{D}(E)$ connecting the occupied π MO's of A and the vacant π MO's of B (including those connecting internally the occupied π MO's of A and those connecting internally the vacant π MO's of B) only, as well as the diagonal elements as illustrated in d, one obtains an energy $E_0 + ESX + CT_\pi$, where CT_π is the charge transfer energy through π orbitals. Similarly, CT_σ can be calculated. Pushing the method still further, if one chooses one particular occupied orbital, say MO_i of A, and includes only the matrix elements connecting this MO to the vacant MO's of B (including those connecting vacant MO's of B internally) as well as all the diagonal elements in the SCF calculation, one can culculate $CT_{Ai\rightarrow B}$, the charge transfer energy from the MO_i of A to B. This extension is now so flexible that one can examine any given orbital interaction. One need only to group orbitals which are to be allowed to mutually interact and include all the matrix elements within each group in addition to the diagonal elements in each SCF cycle. The final energy contains the desired interaction plus E_0 + ESX (or ES, if one uses an integral tape neglecting all the intermolecular differential overlap[12]).

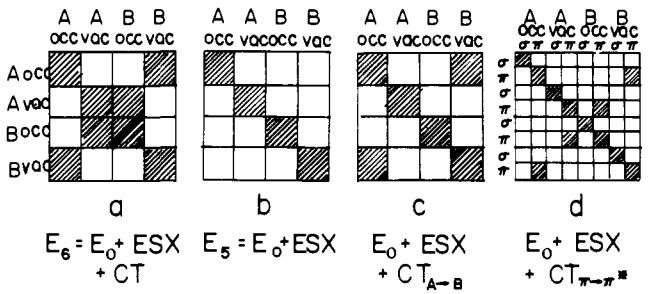

Extra care must be taken for calculation of components of orbital energies. For instance, to calculate the total energy component ES one can either use only the diagonal elements

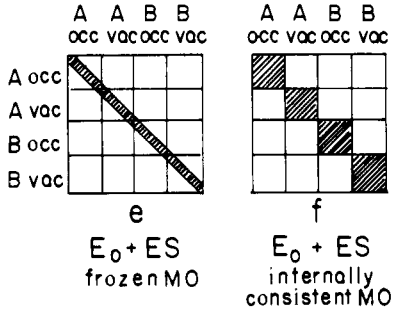

of the Hartree-Fock matrix, as illustrated in e, or the diagonal blocks only, as in f, with the integrals neglecting the intermolecular differential overlap. The two schemes, however, give different orbital energies. The scheme e corresponds to "frozen MO's", that is, the MO's are the same as the MO's of the isolated molecules and their energies reflect the electrostatic potential due to the complexing partner. Scheme f allows the occupied MO's to mix with each other within each monomer and diagonalizes the model Hartree-Fock matrix which reflects the electrostatic potential of the partner. The resultant MO's, therefore, should be called the "internally consistent MO's". This mixing should not be considered as polarization, since it allows mixing only within occupied orbitals of monomer but not between occupied and vacant orbitals and since these MO's give the same total energy as the frozen MO's do. To be concordant with other components which are determined self-consistently, we use the internally consistent MO energies for $E_i^0 + E_{i,ES}$. Actually, the difference between the two ES MO energy components is negligible for $(H_2O)_2$ as studied in the present paper. Similar caution is required for evaluation of the EX component. The total energy component EX does not depend on the manner in which occupied MO's are orthogonalized, whereas the MO component $E_{i,EX}$ does. The diagonalization of the Kitaura-Morokuma model operator including $A_{occ} \leftrightarrow B_{occ}$ and $A_{vac} \leftrightarrow B_{vac}$ blocks as well as the diagonal blocks gives the "internally consistent" $E_{i,EX}$, which is unique. We adopt this $E_{i,EX}$ for the analysis. In addition, MO energy components suffer from further complications. When mixing of MO's is very strong, it becomes impossible to assign a particular orbital to an MO of the isolated molecules. An example is MO 11 and 12 of $(H_2O)_2$ as discussed in section IIIB. In such a case the orbital component analysis loses much of its physical significance.

References and Notes

(1) (a) G. C. Pimentel and A. L. McClellan, "The Hydrogen Bond", W. H. Freeman, San Francisco, Calif., 1960; (b) M. D. Joesten and L. J. Schaad, "Hydrogen Bonding", Marcel Dekker, New York, N.Y., 1974.
(2) (a) J. Rose, "Molecular Complexes", Pergamon Press, Oxford, 1967; (b) R. Foster, "Organic Charge Transfer Complexes", Academic Press, New York, N.Y., 1969; (c) J. Yarwood, "Spectroscopy and Structure of Molecular Complexes", Plenum Press, London, 1973.
(3) (a) R. S. Mulliken, *J. Am. Chem. Soc.*, **72**, 600 (1950); (b) M. W. Hanna, *ibid.*, **90**, 285 (1968); (c) R. S. Mulliken and N. B. Person, *ibid.*, **91**, 3409 (1969).
(4) (a) P. A. Kollman and L. C. Allen, *Chem. Rev.*, **72**, 283 (1972); (b) P. A. Kollman, "Modern Theoretical Chemistry", H. F. Schaefer, Ed., Plenum

Press, New York, N.Y., in press.
(5) K. Morokuma, *J. Chem. Phys.*, **55,** 1236 (1971).
(6) K. Kitaura and K. Morokuma, *Int. J. Quantum Chem.*, **10,** 325 (1976).
(7) (a) S. Iwata and K. Morokuma, *J. Am. Chem. Soc.*, **95,** 7563 (1973), and **97,** 4786 (1975); (b) S. Iwata and K. Morokuma, *ibid.*, **97,** 966 (1975).
(8) K. Morokuma, S. Iwata, and W. A. Lathan, "The World of Quantum Chemistry", R. Daudel and B. Pullman, Ed., D. Reidel Publishing Co., Dordrecht, Holland, 1974, p 277.
(9) S. Yamabe and K. Morokuma, *J. Am. Chem. Soc.*, **97,** 4458 (1975).
(10) W. A. Lathan and K. Morokuma, *J. Am. Chem. Soc.*, **97,** 3615 (1975).
(11) W. A. Lathan, G. R. Pack, and K. Morokuma, *J. Am. Chem. Soc.*, **97,** 6624 (1975).
(12) H. Umeyama and K. Morokuma, *J. Am. Chem. Soc.*, **98,** 7208 (1976).
(13) H. Umeyama, K. Morokuma, and S. Yamabe, *J. Am. Chem. Soc.*, **99,** 330 (1977).
(14) H. Umeyama and K. Morokuma, *J. Am. Chem. Soc.*, **98,** 4400 (1976).
(15) S. Iwata and K. Morokuma, *Theor. Chim. Acta*, in press.
(16) (a) H. Margenau, *Rev. Mod. Phys.*, **11,** 1 (1939); (b) H. Margenau and N. R. Kestner, "Theory of Intermolecular Forces", 2d ed, Pergamon Press, New York, N.Y., 1971; (c) J. O. Hirschfelder, C. F. Curtis, and R. B. Bird, "Theory of Gases and Liquids", Wiley, New York, N.Y., 1964.
(17) (a) B. Jeziorski and M. van Hemert, *Mol. Phys.*, **31,** 713 (1976); (b) H. Lischka, *Chem. Phys. Lett.*, **20,** 448 (1973); *J. Am. Chem. Soc.*, **96,** 476 (1974); O. Matsuoka, E. Clementi, M. Yoshimine, *J. Chem. Phys.*, **64,** 1351 (1976).
(18) C. A. Coulson, *Research*, **10,** 149 (1957).
(19) (a) P. A. Kollman and L. C. Allen, *Theor. Chim. Acta*, **18,** 399 (1970); (b) M. Dreyfus and A. Pullman, *ibid.*, **19,** 20 (1970).
(20) W. J. Hehre, W. A. Lathan, R. Ditchfield, M. D. Newton, and J. A. Pople, GAUSSIAN 70, Quantum Chemistry Program Exchange, Indiana University, 1973.
(21) (a) R. Ditchfield, W. J. Hehre, and J. A. Pople, *J. Chem. Phys.*, **51,** 2657 (1969); (b) W. J. Hehre, R. F. Stewart, and J. A. Pople, *J. Chem. Phys.*, **51,** 2657 (1969).
(22) P. C. Hariharan and J. A. Pople, *Theor. Chim. Acta*, **28,** 213 (1973).
(23) E. Clementi, J. Mehl, and H. Popkie, IBMOL5A, unpublished. Acknowledgment is made to Drs. M. van Hemert and E. Clementi for making the IBMOLH program available.
(24) In our older papers[5,7-11,15], the old method of Morokuma has been used with lower case symbols es, pl, ex, and ct. In newer papers,[6,12-14] the new method of Kitaura–Morokuma is used with upper case symbols ES, PL, EX, CT, and MIX. The new components are equal to the corresponding components, ES = es, PL = pl, and EX = ex, except that CT + MIX = ct. The new method allows the old "charge transfer" term ct to be decomposed further into the true charge transfer term and the coupling term. In this and other newer papers, a negative (positive) value corresponds to a stabilization (destabilization), while in older papers the opposite convention is used.
(25) G. Herzberg, "Spectra of Diatomic Molecules", Van Nostrand, New York, N.Y., 1950.
(26) G. Herzberg, "Electronic Spectra of Polyatomic Molecules", Van Nostrand, New York, N.Y., 1966.
(27) J. D. Swalen, *J. Chem. Phys.*, **23,** 1739 (1955).
(28) P. A. Giguere and I. D. Liu, *Can. J. Chem.*, **30,** 948 (1952).
(29) H. Kim, E. F. Pearson, and E. F. Appelman, *J. Chem. Phys.*, **56,** 1 (1972).
(30) J. E. Wollrab and V. M. Laurie, *J. Chem. Phys.*, **51,** 1580 (1969).
(31) T. R. Dyke and J. S. Muenter, *J. Chem. Phys.*, **60,** 2929 (1974).
(32) A. Johansson, P. Kollman, and S. Rothenberg, *Theor. Chim. Acta*, **29,** 167 (1973).
(33) If the interaction is of a dipole–dipole type, it should be proportional to the square of the dipole moment. The scaling of the dipole moment by a factor γ brings about the scaling in the energy by a factor γ^2. Instead, the present comparison of ES(6-31G**)/ES(4-31G) and μ(6-31G**)/μ(4-31G) yields a linear relationship between the two. This can probably be interpreted as an evidence that the interaction is not a simple point dipole–point dipole interaction. We rather use this linear relationship as an empirical parameter and proceed to use it to scale the energy. An additional posteriori justification is the agreement of ΔE_{scaled} with the best SCF value of Popkie et al. Anyhow, the scaled values should be considered only as a qualitative estimate of the correct values. One should also note that our qualitative conclusions on the nature of hydrogen bonding do not depend on whether one used scaled or unscaled values.
(34) H. Popkie, H. Kistenmacher, and E. Clementi, *J. Chem. Phys.*, **59,** 1325 (1973).
(35) P. Kollman, J. McKelvey, A. Johansson, and S. Rothenberg, *J. Am. Chem. Soc.*, **97,** 955 (1975), obtains $\theta = 37°$.
(36) J. O. Noell and K. Morokuma, *Chem. Phys. Lett.*, **36,** 465 (1975); *J. Phys. Chem.*, **80,** 2675 (1976).
(37) F. Stillinger and A. Rahman, *J. Chem. Phys.*, **55,** 3336 (1971).
(38) K. Morokuma and L. Pedersen, *J. Chem. Phys.*, **48,** 3275 (1968).
(39) P. A. Kollman and L. C. Allen, *J. Chem. Phys.*, **51,** 3286 (1969).
(40) T. R. Dyke, B. J. Howard, and W. Klemperer, *J. Chem. Phys.*, **56,** 2442 (1972).
(41) The same argument has been successfully used to interpret the angular dependence of energy components in H_3N–halogen complexes and $(F_2)_2$ in ref 13.
(42) D. R. Yarkony, S. V. O'Neil, H. F. Schaefer, C. P. Baskin, and C. F. Bender, *J. Chem. Phys.*, **60,** 855 (1974), finds $\gamma = 5°$ with a "double ζ + polarization" basis set.
(43) P. A. Kollman and L. C. Allen, *J. Chem. Phys.*, **52,** 5085 (1970).
(44) G. H. F. Diercksen and W. P. Kramer, *Chem. Phys. Lett.*, **6,** 419 (1970).
(45) As before, the HF distance is assumed to be fixed at the monomer's experimental value. The shape of potential energy curves as the HF distance is stretched will be discussed elsewhere in connection with the solvent effects on the curves in ref 36.
(46) L. C. Allen, *J. Am. Chem. Soc.*, **97,** 6921 (1975).
(47) The calculated δ_X from the Mulliken population is N, −0.93; O, −0.79, and F, −0.48 and δ_H is H_3CH, +0.15; H_2NH, +0.31, HOH, +0.39; and FH, +0.48. The H- - -X distance R_{HX} is taken from Table XVI and the monomer geometry. The relationship between ES and $\delta_X\delta_H/R_{HX}$ is quite smooth, except $(HF)_2$ and $(NH_3)_2$. A less satisfactory but qualitatively still good relationship between ES is also found for the interaction $\delta_X\mu_{HY}/R_{X\mu}^2$ between the bond dipole μ_{HX} (taken from ref 46) and δ_x, where $R_{X\mu}$ is assumed to be the distance between X and the midpoint of the bond HY. These obviously oversimplified models are used here to draw a qualitative picture of ES and are not intended for a quantitative comparison.
(48) (a) K. Morokuma and H. Umeyama, *Chem. Phys. Lett.*, in press; (b) see also a review by L. C. Allen, "Modern Theoretical Chemistry", H. F. Schaefer, Ed., Plenum Press, New York, N.Y., in press.
(49) J. E. Del Bene, *J. Chem. Phys.*, **55,** 4633 (1971); **56,** 4923 (1971); **57,** 1899 (1972); **58,** 3139 (1973); *J. Am. Chem. Soc.*, **95,** 5460 (1973).
(50) (a) P. A. Kollman, J. F. Liebman, and L. C. Allen, *J. Am. Chem. Soc.*, **92,** 1142 (1970); (b) P. A. Kollman, C. F. Bender, and S. Rothenberg, *ibid.*, **94,** 8016 (1972); (c) C. P. Baskin, C. F. Bender, and P. A. Kollman, *ibid.*, **95,** 5868 (1973).
(51) H. Umeyama, K. Kitaura, and K. Morokuma, *Chem. Phys. Lett.*, **36,** 11 (1975).